DIABETES TECHNOLOGY & THERAPEUTICS
Volume 6, Number 5, 2004

Review

Non-Invasive Glucose Measurement Technologies: An Update from 1999 to the Dawn of the New Millennium

OMAR S. KHALIL, Ph.D.

ABSTRACT

There are three main issues in non-invasive (NI) glucose measurements: namely, specificity, compartmentalization of glucose values, and calibration. There has been progress in the use of near-infrared and mid-infrared spectroscopy. Recently new glucose measurement methods have been developed, exploiting the effect of glucose on erythrocyte scattering, new photoacoustic phenomenon, optical coherence tomography, thermo-optical studies on human skin, Raman spectroscopy studies, fluorescence measurements, and use of photonic crystals. In addition to optical methods, *in vivo* electrical impedance results have been reported. Some of these methods measure intrinsic properties of glucose; others deal with its effect on tissue or blood properties. Recent studies on skin from individuals with diabetes and its response to stimuli, skin thermo-optical response, peripheral blood flow, and red blood cell rheology in diabetes shed new light on physical and physiological changes resulting from the disease that can affect NI glucose measurements. There have been advances in understanding compartmentalization of glucose values by targeting certain regions of human tissue. Calibration of NI measurements and devices is still an open question. More studies are needed to understand the specific glucose signals and signals that are due to the effect of glucose on blood and tissue properties. These studies should be performed under normal physiological conditions and in the presence of other co-morbidities.

INTRODUCTION

Non-invasive (NI) glucose measurements

NI DIAGNOSIS AND MONITORING of diabetes attracted tremendous attention in the past 2 decades because of the emergence of diabetes as a major epidemic, especially when associated with the increased overall obesity of the population. NI determination of glucose will promote more frequent testing, allows tighter control of diabetes, and delays the onset of diabetes complications and their associated health care costs.

It is now more than 15 years since the first reports of the feasibility of NI glucose, and close to 5 years since the spectroscopic aspects of NI glucose determinations were reviewed,[1] yet there is no commercialized NI glucose product yet. This paper reviews advances in NI glucose testing methods that were suggested or tested over the period between 1999 and the dawn of the New Millennium. Previously reviewed methods will not be discussed unless new whole blood, animal model, or human experiments have been published. Other review articles have covered various aspects of NI

Diagnostics Division, Abbott Laboratories, Abbott Park, Illinois.

sensing of glucose.[2,3] In addition to the previously reviewed detection technologies,[1–3] new methods that have appeared over the past 4 years will be discussed. The review will concentrate on published, peer-reviewed papers. Discussion of methods disclosed only in patents will be limited. This is because patents have limited data sets and lack the detailed information on experimental design and data analysis that are presented in peer-reviewed papers. Methods that show high correlations with glucose and low estimation errors will be particularly scrutinized as they describe performance close to that of a viable commercial product.

The U.S. Food and Drug Administration may consider NI and minimally invasive devices that are intended to measure, monitor, or predict blood glucose levels in persons with diabetes to be high-risk medical devices subject to pre-market approval.[4] Gutman *et al*.[4] saw that the technology is not yet well understood, and the information obtained from these devices is often different from the information that has been the traditional base for the management of diabetes; consequently the Food and Drug Administration will require both analytical and clinical studies to support the intended claims for these new NI devices. Analytical studies for *in vitro* diagnostic devices generally include study of dose–response relations, determination of factors affecting accuracy and precision, recovery studies, and interference studies in serum and blood samples. Analytical calibration of a home glucose monitor implies determination of glucose concentration from a standard curve generated by using calibrators and standards. It will be difficult to perform these studies for NI glucose devices where calibration will be mainly based on clinical data. It is important to initiate discussions on the possibility of using data obtained on tissue-simulating phantoms and simulation study results to augment clinical data on human volunteers in proving performance of NI glucose testing devices. At least these studies could be used to explain the theory of operation of the device.

There are three main issues in NI glucose measurements: specificity, compartmentalization of glucose values, and calibration. Three questions arise regarding NI determination of glucose:

1. What is actually being detected and determined? Is it an intrinsic property of the glucose molecule, or is it the effect of change in glucose concentrations on tissue or blood properties?
2. In what body compartment is this glucose value determined? How does the determined concentration relate to arterial blood glucose concentration?
3. How to calibrate the NI testing device? Is it a single-person calibration or multiple-person (universal) calibration? Will the NI testing device be calibrated at the factory, or can the user calibrate it? What data inputs are required for the calibration?

Specificity of NI glucose measurements

Methods used for the NI determination of glucose can be classified in two broad categories: as methods tracking a molecular property of glucose, or methods tracking the effect of glucose on tissue and blood properties. The first category depends on tracking an intrinsic molecular property of glucose such as near-infrared (NIR) absorption coefficient, mid-infrared (IR) absorption coefficient, optical rotation, Raman shifts, NIR photoacoustic (PA) absorption, and the like. These methods assume the ability to detect glucose in tissue or blood independent of other body components, and also independent of the body's physiological state. The second set of methods depends on measuring the effect of glucose on the optical properties of tissue. These properties include light scattering coefficient of tissue, refractive index of interstitial fluid (ISF), and sound propagation in tissue.

The ability to collect reliable experimental NI glucose data faces several obstacles: (a) the minute magnitude of the measured signals, (b) repositioning error of the measuring probe with respect to the body part, (c) temperature variations, (d) variations in tissue physical properties at the probe/body interface, (e) efficiency of optical and thermal coupling between the probe and tissue, and (f) effect of

probe/tissue interaction on signal magnitude, etc. Advances in overcoming these obstacles will be discussed in this article.

Compartmentalization of glucose values

Glucose in the human body is found in several body fluids, such as blood, tissue ISF, eye vitreous fluid, tears, and sweat. It is distributed in different body compartments. Current patient care is based on determination of clinically significant concentrations of glucose using *in vitro* invasive reference methods, which involve sampling of venous blood or arterialized venous blood. Glucose is detected either in whole blood or in the separated serum. An enzymatic method with optical or electrochemical sensor is used for subsequent detection. Several NI methods propose determination of glucose in tissue ISF. Glucose in the ISF, or any other body fluid, can be used as a substitute for venous or capillary blood glucose values only if changes in its magnitude and duration of change in the blood vessels and tissue are identical.[5] This may not be the case when changes in blood glucose values are sudden and are too large in magnitude to allow for equilibration between vascular and interstitial levels of glucose.[5,6] Even for blood glucose measurements, there are site-specific effects on the magnitude of the glucose levels.[6] Equilibration between blood glucose values and the glucose concentration in other body fluids, such as the eye vitreous fluid, the ISF, and saliva, has been a controversial issue with widely different reported lag times.

In a study on the human arms as a body site, Thennadil *et al*.[7] used the suction blister technique to investigate the relationship between glucose levels in dermal ISF and capillary venous blood in subjects with diabetes whose blood glucose levels were manipulated so as to induce rapid changes in blood glucose levels. Glucose levels in the three compartments exhibited high correlations when individual volunteers were considered separately, or when data from all volunteers were combined. No significant time lag was observed between ISF and either capillary or venous blood glucose levels during the glucose excursions.[7] However, it was argued that the condition in the previously described experiment allowed for slow equilibration between blood glucose and ISF glucose without large sudden surges in glucose values in either fluid.[6] Lag times between blood glucose levels and ISF glucose levels were reported for implantable glucose sensors.[8,9] ISF glucose concentration lagged behind blood glucose values by 4.4 ± 0.8 min. The relationship between blood and ISF glucose was not affected by insulin. Delays in ISF glucose equilibration could be corrected with digital filters. The authors summarized lag time between ISF and blood glucose values for different technologies: These lag times varied from <5 min to >30 min, depending on the measurement technology.[9]

Several body sites were studied or suggested for the NI determination of glucose, raising the possibility of different values in body compartments for different sites. Forearm skin,[10–12] fingers,[13–16] ear lobe,[17,18] tongue,[19] abdominal tissue,[20] inner lip mucosa,[21] the eye,[22] and the conjunctiva[23] were suggested or used as sites for NI glucose measurements. Different delay times between blood glucose values and NI-determined glucose have been suggested, and may be encountered, for different body sites.

Calibration of NI measurements

Multivariate analysis is generally used for determination of the concentration of a component in a complex mixture.[24–26] It has been used for data analysis of NI glucose measurements that are based on NIR spectra.[12,15,19,21] The quality of an NI measurement is judged mainly by the magnitude of the standard error of prediction (SEP) and the prediction correlation coefficient (R_p). A low SEP, when associated with a high correlation coefficient, is indicative of a successful determination. One must guard against the possibility of (a) small range of concentration of analytes, (b) chance correlation with other time-dependent events, and (c) overfitting the experimental data. Extreme care must be taken to avoid the effect of overfitting. The training set and the prediction set need to be separated in time. The number of input NI data points, such as spectra, temperatures, distances, etc., must be larger than the number of terms in the fitting equations. Partial least

squares (PLS) calibration models require use of several independent standard spectra for each factor used in the PLS analysis.

A high SEP can be interpreted in one of three ways: (a) The calibration model is void of glucose-specific information, (b) glucose predictions are limited by measurement noise, or (c) glucose predictions are limited by biological background noise in the body part and repositioning errors of the probe with respect to the body part. Noise sources, such as circulation parameters, skin surface condition, skin water content, circadian rhythm effects, and temperature changes, are examples of biological variables that have not been yet considered in sufficient detail.

A simple method to establish a calibration model is to fit the measured NI experimental data to invasively determined glucose concentrations. Linear least squares (LLS) fitting or PLS fitting is used. For example, a linear calibration relationship can have the form[11,12,15,19,21]:

$$[\text{Glucose}] = a_0 + \Sigma_i\, a_i \times P\ (k,l,m) \qquad (1)$$

where [Glucose] is the concentration of glucose, a_i is a regression coefficient, P is a measured parameter, and k, l, and m are various constraints, which may be different wavelengths, wavelengths and distances, wavelengths and temperatures, etc. The calibration correlation coefficient (R_c) and the standard error of calibration (SEC) are then determined. The calibration model can then be validated by checking its ability to predict one data point using the rest of the data points as the calibration set. The process is repeated for each data point in the set. This is known as the leave-one-out cross validation (LOOCV). The predicted values and the reference values are then used to calculate the standard error of cross-validation prediction (SECV) and the cross-validation correlation coefficient (R_{CV}). A low SECV and a high R_{CV} indicate the validity of the calibration model. These R_{CV} and SECV values can be used, with caution, to indicate the prediction ability of the model. This should be especially the case when only a small number of data points are available. As the LOOCV procedure involves the use of data points from the same experimental set, it is prone to effects of spurious correlations with instrument or with experimental time-dependent events. True prediction can only be achieved by using independent calibration and prediction data sets that have been obtained over different time periods. The two calculated prediction parameters are the R_p and the SEP.

A major difference between *in vitro* and *in vivo* calibration experiments is that the human body has time-dependent physiological effects that are apparent in the circadian rhythm. In a resting state the cardiac pulse, blood pressure, blood circulation, respiration, body temperature, and cutaneous blood flow are subject to circadian periodicity. These parameters are at their highest values between 8 a.m. and 12 noon, and again between 4 p.m. and 7 p.m. They are at their lowest values between 1 p.m. and 3 p.m., and again between 10 p.m. and 6 a.m., next morning. This regular periodicity for normal healthy individuals is perturbed by changes in environmental conditions, and certain diseases.[27,28] In the meantime, the concentration of glucose in subjects without diabetes and patients with in-control diabetes varies during the day and follows a regular profile. Generally, the morning glucose values are low (fasting glucose), levels increase substantially after the morning meal, decrease to a pre-mid-day nadir, increase again after midday and evening meals, and settle to lower values at night. This profile will be distorted in cases of advanced diabetes. Deviation from this pattern requires intervention. Tight glycemic control can return the daily glucose fluctuation pattern close to that of a healthy individual. Glucose injection produced body temperature (vital sign) changes.[29] There is a potential for a coincidental correlation between the circadian fluctuation of glucose concentration in human blood and the circadian periodicity of the body temperature and other vital signs. It is important to separate the effects of circadian body temperature and blood flow effects on the NI measurement so they do not confound the signals used to calculate blood glucose concentration.

Calibration of NI glucose devices requires the availability of various invasively determined concentrations of glucose and the correspond-

ing NI signals. One calibration approach is to induce a change in glucose concentration spanning a range over which the *in vivo* measured signal can be monitored. This is achieved by using a glucose clamp procedure,[30–32] an oral glucose tolerance test (OGTT), or a meal tolerance test (MTT). In the glucose clamp experiment, the concentrations of injected glucose and insulin are manipulated to result in a steady concentration of either glucose (hyperglycemic or hypoglycemic clamps) or insulin (hyperinsulinemic clamp) over a period of time. In the OGTT a known load, typically 75 g of glucose, is given to a fasting subject, and the concentration of glucose is followed as a function of time. The MTT is similar to the OGTT, except that the carbohydrate load is administered as a meal rather than a glucose load. Data that are generated during the test period can be used to predict glucose concentration from subsequent NI measurements. As the response of an NI instrument may embody non–glucose-related physiological effects, relying on calibration based on correlating OGTT or MTT data with NI instrument response leads to a calibration model that is unique to the individual tested. This calibration model will need to be periodically updated, using an invasive test. Time-dependent artifacts can influence the results from multivariate calibrations when randomized sampling over time cannot be performed. In addition to instrument-related time variables, the previously discussed circadian rhythm of the human body can lead to spurious time-dependent biological background that will be superimposed on the sequential MTT data points. Although OGTT and MTT data are needed to prove that a particular NI signal varies with induced change in glucose concentration, they are not sufficient to establish a reliable calibration of signal versus blood glucose values. Ideally, it is preferable to have a self-calibrating technology that does not require multiple invasive data points to calibrate the device, the calibration of which is not unique to an individual.

A calibration method that is more immune to time-dependent effects is a random spot test that is performed at randomized time slots during the day and over a long period of time (longitudinal study).[19,33,34] This approach allows the use of data points that cover multiple physiological conditions and avoids circadian rhythm-related correlations. It will avoid most instrument-related chance correlation.[33]

Frequent recalibration of a NI device with an invasive test is a major issue. The higher the frequency of these invasive recalibrations, the lower is the value of the NI testing device for the patient. An NI device that depends on frequent invasive recalibration, even when technically successful, will doubtfully be accepted in the market. The term "universal calibration" has been touted as an achievable goal, but current sensitivity and specificity of the available methods preclude this assertion. After establishing specificity of the test method and understanding the compartmentalization of glucose values, which are essential to the technical feasibility of a test device, researchers should address calibration frequency issues, as it is important to the patient's acceptance of an NI testing product.

OPTICAL PROPERTIES OF TISSUES AND HUMAN SKIN

NIR tissue optical properties

The NIR spectral region is commonly used in most reported methods. It has several spectral windows where hemoglobin, melanin, and water absorption band intensities are low enough to allow light to penetrate in the tissue, which enables NI spectral measurements.

Attenuation of light in tissue is described, according to light transport theory, by the effective attenuation coefficient μ_{eff}[35]:

$$I = I_0\, e^{-\mu_{eff} l} \tag{2}$$

where I_0 is the incident light intensity, I is the reflected light intensity, l is the optical pathlength in tissue, and μ_{eff} is defined as:

$$\mu_{eff} = [3\ \mu_a\ (\mu_a + \mu_s')]^{1/2} \tag{3}$$

An exact solution of light transport equation in turbid media can be modeled by following the path of each individual photon and calculating the probability of scattering or absorption in a series of steps using Monte Carlo sim-

ulation.[35] This modeling is used to study the path of photons in tissues and was used for optimization of photodynamic therapy,[36] laser-Doppler flowmetry (LDF),[37] and optical mammography.[38]

Light propagation in tissue is expressed by the absorption coefficient, μ_a, and the scattering coefficient, μ_s'. Absorption and scattering coefficients of tissue are determined by performing one or more of transmission, diffuse reflectance, localized reflectance, time domain, or frequency domain measurements.[35] The absorption coefficient is related to the concentration of a tissue chromophore by $\mu_a = 2.303\ \varepsilon C$ cm^{-1}, where ε is the molar extinction coefficient and C is the molar concentration. Changes in glucose concentration can influence μ_a of tissue through absorption corresponding to water displacement (absorption decreases as glucose concentration increases), or change in its intrinsic absorption (absorption increases as glucose concentration increases). Change in μ_a due to water displacement is nonspecific. The μ_a of glucose in the NIR is low and is much smaller than that of water by virtue of the large disparity in their respective concentrations. In the NIR the weak glucose overtone and combination spectral bands overlap with other stronger overtone and combination bands of water, hemoglobin, protein, and fats.[1]

An example of the magnitude of NIR glucose intrinsic absorption signals is illustrated by the values of the extinction coefficient of glucose. Youcef-Toumi and Saptari[39] determined ε of glucose at the first overtone band 1,686 nm (5,930 cm^{-1}) and the combination band 2,273 nm (4,430 cm^{-1}). The measured value at 1,689 nm was $2.3 \times 10^{-2}\ M^{-1}\ cm^{-1}$, and that measured at 2,257 nm was $0.4\ M^{-1}\ cm^{-1}$. The values are far smaller than the $6.2 \times 10^{3}\ M^{-1}\ cm^{-1}$ ε value of NADH at 340 nm, a compound that is usually used for the determination of serum glucose values on automated blood analyzers. Using a 1-mm pathlength, a 10 mmol/L glucose concentration will generate an absorbance value of 2.3×10^{-5} absorbance units at 1,686 nm and 4×10^{-4} absorbance units at 2,257 mm. A 1-mm pathlength is longer than the pathlength encountered in diffuse reflectance measurements, and is of comparable magnitude to the pathlength in some spatially resolved reflectance measurements.[10,11] The intrinsic extinction coefficient of glucose will be much lower at the higher overtone bands between 800 nm and 1,300 nm, thus requiring extremely sensitive detection and elimination of sources of background noise, and leading to extreme difficulty in interpreting the data in this spectral range.[39]

The scattering coefficient is $\mu_s' = \sigma\rho\ [1 - g]$ cm^{-1}, where σ is the scattering cross section, ρ is the number density of scattering centers, and g is the anisotropy factor.[35] Change in glucose concentration affects the intensity of light scattered by tissue. The reduced scattering coefficient of a tissue or can be expressed as $\mu_s' = f(\rho, a, n_{scatterer}/n_{medium})$, where ρ is the number density of scattering centers in the observation volume, a is the mean diameter of scattering centers, $n_{scatterer}$ is their refractive index, and n_{medium} is the refractive index of the surrounding fluid.[40] For the case of cutaneous tissue, connective tissue fibers are the scattering centers. Erythrocytes [red blood cells (RBCs)] are the scattering centers for the case of blood. The effect of a solute on the refractive index of a medium, and hence μ_s', is nonspecific and is common to other soluble analytes.

Mid-IR properties of tissue and skin

Mid-IR lies in the spectral range between 2.5 μm (4,000 cm^{-1}) and 10 μm (1,000 cm^{-1}). Bands in this spectral range correspond mainly to frequencies of fundamental molecular vibrations, which are characteristic of the specific chemical bonds. While the NIR spectral range encompasses combinations and overtone bands that are broad and weak, bands in the mid-IR are sharp and have a higher absorption coefficient. The mid-IR spectral bands of glucose and other carbohydrate have been assigned and are dominated by C-C, C-H, and O-H stretching and bending vibrations.[41] The 800–1,200 cm^{-1} fingerprint region of the IR spectrum of glucose has bands at 836, 911, 1,011, 1,047, 1,076, and 1,250 cm^{-1} that have been assigned to C-H bending vibrations.[41,42] A 1,026 cm^{-1} band corresponds to C-O-H bend vibration.[42] Spectral measurements in this frequency interval were used to determine of glucose in serum and blood. IR emission in the

same frequency range was used for NI measurement of glucose and will be discussed later.

Tissue optical properties in the mid-IR between 2.5 μm (4,000 cm^{-1}) to 10 μm (1,000 cm^{-1}) differ from the NIR as scattering decreases at longer wavelengths and light attenuation by water, proteins, and fats absorption spectra dominates. Water constitutes 70% of hydrated tissue, followed by the connective tissue proteins and lipids. The strong absorption limits light penetration depth in tissue to 0.2 μm at 2.5 μm (4,000 cm^{-1}) and to 1.2 μm at a wavelength of 10 μm (1,000 cm^{-1}).[43] Attenuated total reflectance zinc-selenide prisms have been used for studies of the mid-IR spectra of tissue.[21,43–46] Light penetration depth limits the sampling depth to the stratum corneum (SC). Attenuated total reflectance (ATR) mid-IR spectroscopy was used to study properties of the SC such as its water content, and effect of cleansing, stripping the SC by adhesive tape, and partial occlusion on its optical properties. It was also used to study diffusion of topical medication in the SC, and epithelium layers of oral mucosa and other tissues. The results of these studies are quite important for the NI determination of glucose as they reveal several important factors about skin–probe interaction, properties of different skin sites, and effect of skin cleaning procedures on its optical properties.

The mid-IR spectrum of the skin as determined by ATR accessories showed overlap between IR bands of glucose and those in skin components.[43–46] Table 1 summarizes the low-frequency vibrations in the mid-IR band frequencies of water, glucose, and human skin. Although bands in the 10 μm range are specific to glucose in aqueous solutions, there is a high probability of having C-C, C-H, and C-O bending vibrations from other skin components coinciding with them. The C-C bands in the spectrum of skin do not relate only to glucose, as it is a minor component compared with proteins and fats.

Table 1. Mid-IR Frequency Bands (in cm^{-1}) of Water, Glucose, and Human Skin in the Fingerprint Region of Glucose IR Spectrum

Water[a]	*Glucose*[b]	*Skin*[a]
	836	
		852
	911	917
	1,011	
	1,026	1,035
	1,047	
	1,076	1,077
		1,118
1,150		1,164
	1,250	1,245

[a]From Lucassen *et al*.[44]
[b]From Vasko *et al*.[41,42]

Skin mid-IR spectrum depended on its water content, showing increase in intensity in water bands intensity upon hydration.[44–46] Increase of skin hydration was observed upon treating the skin with 70% isopropanol, occlusion of the skin, or tape striping of the skin. Contact between the skin and the probe caused occlusion and increased water content by trapping the transdermal transpired water between the stratum corneum and the probe. This effect should be also present in NIR measurements. It is noticeable in mid-IR ATR studies of skin because of the ability of the technique to sample the SC only without interference from the underlying layers, and because of the sharpness of mid-IR absorption bands.

Diabetes and microcirculation changes

Diabetes mellitus affects microcirculation and leads to microvessel complications such as neuropathy, retinopathy, and nephropathy. LDF studies showed impaired circulation in patients with diabetes, which was manifested by a decrease in cutaneous blood flow[47] and a difference in blood flow response to cooling or warming.[48,49] Vascular walls in the cutaneous microvasculature of patients with diabetes were abnormally thick,[50] and blood vessels responded subnormally to heat, injury, and histamine.[51–53] Persons with type 2 diabetes or borderline glucose intolerance have stiffer arteries than their counterparts with normal glucose tolerance.[54] Patients with diabetes exhibited differences from those without diabetes in cutaneous blood flow,[52–55] reduced maximal hyperemia,[56] impaired peripheral vasomotion,[57] and response to contralateral cooling.[58] Endothelium-dependent vasodilatation is impaired during acute hyperglycemia,[59] and both microvascular and macrovascular reactivities

are reduced in persons at risk for type 2 diabetes.[60] Diabetes causes changes in cutaneous vascular response to external stimuli, which can precede clinical symptoms of diabetes.[61]

In addition to the vascular effects of diabetes, both insulin and glucose are reported to have vascular activities. Acute hyperglycemia attenuated endothelium-dependent vasodilatation in humans.[62] Insulin is reported to cause vasodilatation in human circulation.[63] In another study, acute hyperglycemia (11.78 mmol/L, 212 mg/dL glucose) and hyperinsulinemia (119 μU/L insulin) enhanced vasodilatation in type 1 diabetes over a standard of 4.78 mmol/L (86 mg/dL) glucose and 22 μU/L insulin as shown in Figure 1, which is calculated from the data presented by Oomen *et al*.[64] If one considers the glucose clamp part of the experimental data in Figure 1, *i.e.*, the first two sets of bars show blood flow increases with increasing glucose concentration.[64] Comparing the third set of bars to the first set of bars shows that insulin has a similar effect on cutaneous blood flow as glucose does, and hence on the LDF signals.

The vasodilatory effect of hyperinsulinemia is well established by plethymography of the forearm in both healthy volunteers and subjects with type 1 diabetes.[63,64] These effects were found to be temperature dependent and to vary from site to site in the human body. The resulting increase in light absorption associated with increased perfusion could be erroneously attributed to, and correlated with, blood glucose concentration. Indeed, one patent suggested use of LDF for NI determination of glucose without presenting any experimental data to show potential performance.[65] Such a proposition is suspect in light of the experimental data on the clamp experiments.[64] Hemoglobin electronic absorption spectral bands and water vibration overtone bands dominate the short wavelength NIR spectral window of 600–1,300 nm. The NIR absorbance curve of a finger shifted downwards on restriction of blood flow. It shifted upwards with thermal stimula-

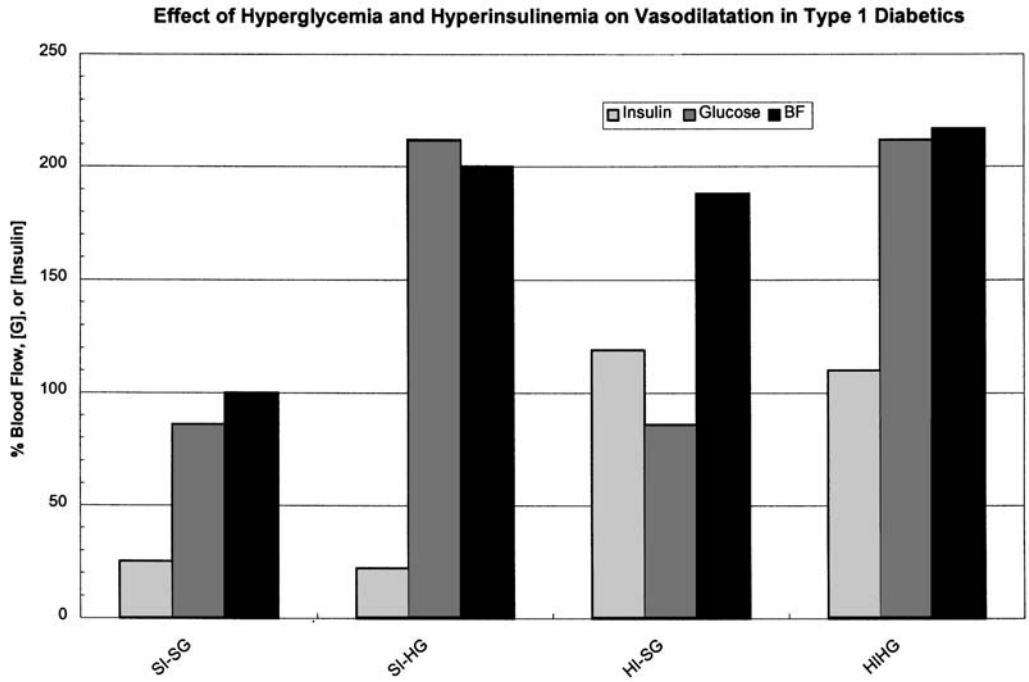

FIG. 1. Results of LDF study on human skin. Data are from Oomen *et al*.[64] and are plotted as the mean values of glucose concentration, insulin concentration, and LDF relative to the standard state. Glucose concentrations were converted to mg/dL for the purpose of graph scaling. The *y*-axis is the relative blood flow (BF), glucose concentration [G] (in mg/dL), or insulin concentration (in mU/L). The *x*-axis is standard insulin/standard glucose (SI-SG), standard insulin/high glucose (SI-HG), high insulin/standard glucose (HI-SG), or high insulin/high glucose (HI-HG). Standard insulin concentration was 22 mU/L, standard glucose concentration was 86 mg/dL (4.78 mmol/L), high insulin concentration was 119 mU/L, and high glucose concentration was 212 mg/dL (11.78 mmol/L).

tion and with post-occlusion hyperemia.[66] The blood flow-induced shifts in the absorbance curve were particularly pronounced in the range of 850–970 nm. LDF-determined skin blood flow correlated with the absorbance values, $R_c = 0.69$.[66] NIR signals between 590 and 1,000 nm correlated with hemoglobin concentration or hematocrit values, resulting in good calibration and prediction errors for either of the two blood parameters.[67,68]

A sudden rise and fall of glucose or insulin concentration, as in the case of the clamp experiment, will lead to vasodilatation and increased perfusion in the outer vascular bed. Blood perfusion will contribute to change in transmission and reflectance signals, especially in the short wavelength NIR range <1,300 nm. Blood perfusion effects can confound correlating the NIR signal change with glucose concentration. This assertion suggests that absorption-based methods, which depend on direct measurement of transmission and reflectance in the short wavelength NIR range, without considering perfusion, are not likely to present a viable approach to NI glucose measurements. Correlating glucose concentration with the optical signal in an MTT experiment assumes that glucose concentration is the only time-dependent variable. Other factors, such as temperature, blood perfusion, tissue compression, blood oxygenation, cutaneous water, and other metabolites or medications that affect tissue blood dynamics, are not usually considered in analyzing NI signals, though they may dominantly affect the measured signal change.

Diabetes and change in tissue (skin) structural properties

In addition to circulation differences between individuals with and without diabetes, a number of dermatological and skin structural factors are associated with diabetes.[69] Among these dermal structural effects are diabetes "thick skin" and diabetes "yellow skin," which may relate pathophysiologically to accelerated collagen aging, elastic fiber fraying, and increased cross-linkage glycosylation of collagen fibers. Monnier *et al.*[70] reported change in dermal collagen structure in patients with diabetes and showed that the level of collagen glycation was associated with the level of glycated hemoglobin (HbA1c). X-ray diffraction studies showed structural changes in collagen skin fiber as a result of diabetes.[71] Light reflected from the skin of individuals with diabetes will have a different intensity and a different response to glucose concentration depending on the extent of structural differences induced by glycation.

Diabetes and blood cell morphology

RBC aggregation is a complex phenomenon that has been widely studied. RBCs aggregate at low blood flow conditions. RBC aggregation is important to microcirculation and is a major factor that contributes to changes in blood flow properties.[72–75] There are reports of differences in refractive index of RBCs and in their aggregation patterns between individuals with and without diabetes.[76,77] This difference affects blood flow and light scattering by RBCs. The combined effects of diabetes on the structure of cutaneous fibers and on RBC aggregation can lead to a difference in transmission, diffuse reflectance, and localized reflectance signals of blood-containing tissues. RBC aggregation is also affected by the concentration of other blood components as triglycerides and cholesterol.[78–80] It depends on other pathological conditions that are associated with low-flow states or change in cell membrane properties. These pathological conditions include diabetes, trauma, ischemia, elevated plasma fibrinogen, hemoglobinopathies, oxidative stress, inflammation, unstable angina, acute myocardial infarction, and bacterial infection.[81,82]

Temperature dependence of optical properties of human skin

Our group recently studied the optothermal properties of human skin within a 2-mm depth in tissue. Temperature change affected μ_a, μ_s', and light penetration depth in cutaneous tissue.[83–87] The effect of temperature on μ_s' was attributed to changes in n_{ISF}. The effect of temperature on μ_a was attributed to its effect on blood perfusion to outer skin layers. Light penetration depth in skin increased by lowering skin temperature.[85–87] Change in light penetra-

tion depth with temperature and wavelength can help targeting a particular cutaneous layer.[85–87] Cooling the cutaneous tissue decreases μ_s' in a manner similar to increasing glucose concentration. Cooling decreases μ_a in a manner similar to decreasing insulin or glucose concentration (decreases cutaneous perfusion). Heating the cutaneous tissue increases μ_s' in a manner similar to decreasing glucose concentration. Heating also increases μ_a in a manner similar to increasing glucose or insulin concentration (increases cutaneous perfusion).

There were noted differences in the values of the optical parameters of skin from persons with and without diabetes. The fractional change in localized reflectance as a result of temperature change was used in combination with a nonlinear discriminant function to classify volunteers into those with and without diabetes,[85–87] which suggested dependence of tissue optical and thermal properties on the diabetes status of an individual. Light scattering by capillary RBCs depends on n_{RBC}/n_{plasma} and will vary with temperature, and can contribute to the observed thermo-optical behavior of skin from subjects with diabetes. The previously mentioned blood circulation differences,[47–58] the skin structural effects,[69–71] and the effect of diabetes on blood flow and rheology[72–77] may have manifested themselves in the observed discrimination between those with and without diabetes in those studies.[85–87]

Discrimination between individuals with and without diabetes on the basis of skin thermo-optical response can be used as an NI screening method of the diabetes status or to assess the extent of complications. An NI screening method can replace multiple glucose tests, HbA1c determination, and probably an MTT or OGTT. Temperature modulation of optical properties of human skin was used in a set of meal tolerance experiments to track glucose changes in human subjects.[11]

Nature of glucose NI measurement's optical window

The outermost layer of the body part is the optical window for an NI measurement. Skin layers, oral mucosa, and the eye lens are optical windows through which an NI glucose measurement is performed. Variation in their properties from person to person, and difference from time to time for the same person, will affect the reproducibility of the optical measurement. Change in the characteristics of the optical widow as a result of interaction with the measuring probe, effect of temperature, and variations in optical and thermal coupling between the probe and the window will affect the reproducibility of the optical measurement. Transepidermal water loss is a characteristic of living skin.[88] Prolonged contact between probe and skin causes local occlusion and limits the escape of water molecules, and can lead to increased hydration of the SC. Hydration of the SC reaches a constant value of 70%[43]; excess water may then appear as a thin layer between the skin and the probe. Transepidermal water loss may cause a time-dependent change or a drift in the measured optical signal, especially in diffuse reflectance measurements. Blank *et al*.[89] used local occlusion to homogenize the effects of different levels of skin dryness on the optical signal.

The results of the thermo-optical studies on human skin suggest that because of blood circulation differences and skin structural effects, skin from an individual with diabetes contributes to the measured signal in a manner different from skin from an individual without diabetes.[83–87] Thus, skin does not act as a passive optical window for an NI glucose measurement. Differences in skin properties and their dependence on disease state or environmental conditions should be taken into consideration in analyzing NI optical signals.

OPTICAL METHODS FOR NI TISSUE MEASUREMENTS

NIR transmission and reflectance

NIR transmission and reflectance NI measurements of glucose are predicated upon the premises that glucose-specific information is embedded within the NIR spectra and can be extracted by using multivariate analysis methods. Study of several body sites (webbing, tongue, upper lip, lower lip, nasal septum, and cheek) for suitability for NIR transmission mea-

surements based on the water and fat contents suggested the tongue as the body part with the lowest fat content.[90] Burmeister *et al.*[19] studied NIR (7,000 and 5,000 cm^{-1}, 1,430–2,000 nm) transmission through the tongue of five subjects with type 1 diabetes over a period of 39 days, performing five measurements per day. The tongue was selected because it is highly vascularized, it does not have an SC, it has little fatty tissue, it is a homogeneous body part, it has a nearly constant temperature, and it offers an aqueous effective pathlength between 5 and 6 mm. Spreading the data collection over several weeks (a random series of spot tests) instead of an OGTT or MTT alleviates contamination of the data set with temporal effects. PLS calibration models were generated for the different individuals. Models were used to predict blind sample concentration (each fifth measurement) or the later part of the data with SEP >3 mmol/L and R_p varying from person to person. Both sets of prediction data points were obtained at different days.

Determination of glucose in oral mucosa using a diffuse reflectance technique was extensively discussed in previous work and in more recent work from Heise's group.[91,92] The wavelength range used was 1,111–1,835 nm. Light penetration in tissue in diffuse reflectance measurements is limited, leading to a short light pathlength. The low extinction coefficient of glucose in this region makes for a very small signal change. The oral mucosa was selected because it is highly vascularized and it does not have an SC layer. One may argue that in spite of the short penetration depth, light is sampling the vascular mucosal bed. Glucose was assumed to be determined in the blood vessels of mucosal tissue. The lowest SEP was 2.1 mmol/L. The medium through which light is transmitted and reflected differs from skin and tissue used in other studies. There is a potential for a lag time between glucose concentration in blood and saliva. Saliva components and residual food in the mouth present sources of interference in this measurement.[1]

Gabriely *et al.*[15] used the NIR reflectance of the thumb, in the 400–1,700 nm range, for NI determination of glucose in a set of insulin and glucose infusion experiments. The thumb was selected because it is highly vascularized. PLS was used for data fitting. Exceptionally high correlation coefficients (R_p >0.95) and exceptionally low SEP (<0.28 mmol/L) were reported.[15] An objection was raised that the prediction set and the calibration set were not independent.[93] A rebuttal indicated that the prediction set had masked samples from the total set that were not used in the calibration model.[94] The prediction error values are vastly smaller than those reported for other NI-NIR techniques, for *in vitro* glucose results in a much simpler media, and even for some commercial invasive home glucose meters. These small SEP values are quite encouraging, unless there is overfitting in the data analysis, which warrants a thorough review of this work. There are some questions that are not clearly answered,[15] for example:

1. *Reference measurements*. Did the reference measurement contribute to signal quality?
2. *Body interface*. Was the optical probe in contact with the thumb all the 5-h experiment time? Were the measurements performed intermittently? What was the magnitude of the repositioning error of the thumb? What was the applied pressure by the measurement fixture? Was there any occlusion due to the applied pressure?
3. *Wavelength*. Were the 10–27 factors in the PLS regression analysis individual wavelengths or spectral bands? Which wavelengths in the 400–1,700 nm range were used in the PLS fitting? How many independent spectra were used per PLS factor? Which portion of the spectrum contributed to the correlation? Did the hemoglobin absorption bands contribute to the correlation?
4. *Timing*. Did the experiment time overlap with one segment of the circadian rhythm and one time window for the instrument? Chance correlation between instrument parameters and time contributed to sequential *in vitro* measurements of glucose.[33]

The issue of independence of prediction data set from the calibration set was debated.[93,94] The masked experiment data points that represented the prediction set were not included in the calibration set.[94] They are still a part of the events in the same time sequence for each

clamp experiment, which makes them follow the same time dependence of whatever parameter that is changing during the experiment. Data sets used in the calibration model and data sets used for testing prediction should be obtained in separate clamp experiments. An example would be using the calibration model from one day to predict clamp experiment results from another day. A more direct approach to avoid chance correlation, and to account for repositioning errors, is to test randomized set of spot tests.[19] The small SEP obtained in the study by Gabriely *et al.*[15] can be very encouraging and warrants repeating the experiment on a number of individuals to confirm the published data and to answer the questions about experimental design and data analysis. If the SEP values are still as low as reported,[15] this can present an important step towards the NI-NIR optical detection of glucose.

Maruo *et al.*[10,95] reported a NI glucose determination method based on NIR absorption at the overtone bands of glucose. A 200-μm illuminating optical fiber in touch with the skin delivered polychromatic light. Reflected light was collected at a distance 0.65 mm from the illumination point using a second 200-μm fiber. Collected light was analyzed by a spectrometer as absorption spectra in the wavelength range 1,500–1,800 nm.[10,95] This optical arrangement restricted the sampled depth to 0.5–2 mm to encompass the dermis. It avoids the SC and epidermis on the top, and the adipose tissue at the bottom of the dermis layer. The measured absorbance ($-\log_{10}$ reflected intensity) was fitted to the *in vitro* glucose data to generate a calibration model. Two subjects without diabetes were tested, with six OGTTs performed. Five of these tests were used in the calibration model, and the sixth set was predicted for each person from his own calibration set; the SEP was 1.4 mmol/L. There was a run-to-run bias of up to 5.6 mmol/L. This bias was attributed to site structural differences.[95]

Using PLS fitting and the formalism given in Eq. 1, Maruo *et al.*[95] found that the largest value for the regression coefficient was at ~1,600 nm. A similar positive regression coefficient was found at the same wavelength when glucose was determined in serum using Fourier transform IR. Maruo *et al*.[95] used this as an evidence of specificity, *i.e.*, the signal at 1,600 nm is due to NIR absorption by glucose molecules. One control experiment was performed where the subject drank cold water, and no glucose was predicted by this subject's measurement.

In a longitudinal study, Samann *et al*.[34] reported the long-term accuracy and stability of diffuse reflectance of human finger over the 800–1,350 nm spectral range. Spectra of 10 patients with diabetes were evaluated. Individual calibration models were calculated for each patient from the spectra, which were recorded at the beginning of the investigation. These models were then applied to calculate blood glucose values from subsequently obtained spectra, which were recorded 84–169 days later. The long-term accuracy and stability of the calibration models, expressed as the root mean squared error of prediction, varied from 3.1 to 35.9 mmol/L. The results show the need to improve the long-term stability of the detection and calibration method, and to understand the underlying physiological processes over time.

NIR diffuse reflectance of the arm was measured for several bands in the 1,050–2,450 nm spectral range and was correlated with glucose concentration.[89] Precautions were made to minimize data variability due to skin hydration, variations in tissue temperature, and probe contact pressure. In a first approach, seven volunteers with diabetes were studied over a 35-day period with random collection of NIR spectra. The second approach involved three volunteers without diabetes and the use of OGTT over multiple days. Statistically valid calibration models were developed on three of the seven volunteers with diabetes. The mean SECV was 1.41 mmol/L. The results from the OGTT testing of the three volunteers without diabetes yielded an SECV of 1.1 mmol/L. Validation of the calibration model with an independent test set produced a mean SEP equivalent to 1.03 mmol/L. This group studied calibration transfer between instruments and between persons and the stability of calibration over extended time periods. It was possible to establish a standardized algorithm for nine out of 139 subjects.[89]

A summary of data on glucose NIR absorbance measurements in human experiments

is given in Table 2, which describes the specificity, compartmentalization, and calibration status of each method discussed.

Mid-IR spectroscopy

A different approach is to examine the fundamental frequencies of glucose is the mid-IR. Janatsch *et al*.[96] used mid-IR spectral analysis of human blood plasma with an ATR cell. The concentrations of total protein, glucose, triglycerides, total cholesterol, urea, and uric acid were measured by chemical or enzymatic methods. For these constituents a PLS algorithm was used for a multivariate calibration, including the IR fingerprint region of the plasma spectra. The average cross-validation prediction SECV for glucose was 1.2 mmol/L.[96]

Deissel *et al*.[97] determined glucose using mid-IR spectroscopy and ATR measurement. Dried glucose films from small volume (100-nL) aqueous glucose solutions were deposited on an (ATR) accessory of a Fourier transform IR spectrometer equipped with a pyroelectric detector. Quantification of glucose was achieved between 0.6 and 33 mmol/L in samples with volumes as low as 7 nL. The SEP for the concentration range 0.6–5.6 mmol/L was 0.18 mmol/L, with full interval data between 1,180 and 940 cm^{-1}. When all samples within the whole concentration range to 33 mmol/L were included, the SEP increased to 1.1 mmol/L because of a nonlinear signal dependence on glucose concentration.[97]

Petrich *et al*.[98] correlated the shape of the mid-IR spectra (1,000–4,000 cm^{-1}) of dried serum samples with the disease state of those with type 1 or type 2 diabetes and without diabetes. These investigators applied cluster analysis and discriminant analysis to the data. Approximately 80% sensitivities and specificities of the disease state were achieved within their data set.[98] Spectral features in the mid-IR spectrum 1,119–1,022 cm^{-1} (8.937–9.785 μm) were used for measurement of glucose in whole blood.[99] Another mid-IR determination glucose in whole blood in the range 950–1,200 cm^{-1} (8.333–10.526 μm) yielded an SEP of 0.59 mmol/L.[100]

A comparison of the performance of NIR and mid-IR spectral measurements is presented in the work of the Sandia Group. Haaland *et al.*[101] used NIR spectroscopy to determine glucose concentration in whole blood using a 1-mm cell and PLS for data analysis; PLS-SECV was 1.8 mmol/L over a range of 0.17–41.3 mmol/L in blood and glucose-spiked blood. Ward *et al.*[102] measured in the mid-IR with blood from six subjects with diabetes. In one experiment the blood was spiked with glucose in the range 2.8–25 mmol/L. The second set of samples was postprandial blood obtained from the same subjects during an MTT that had a glucose range between 5.87 and 20.9 mmol/L. PLS-SECV was 0.61 mmol/L for the spiked samples and 0.72 mmol/L for the postprandial blood samples.[102] These data indicate that mid-IR spectral measurements yield lower SECV val-

Table 2. Glucose NIR Absorbance Measurements in Human Experiments

Method	*Reference*	*Specificity*	*Compartmentalization*	*Calibration*
Transmission through tongue	Burmeister *et al*.[19]	Glucose NIR 1,430–2,000 nm	Tongue tissue and blood vessels	Spot test, calibration, prediction SEP >3 mmol/L
Reflectance of oral mucosa	Heise *et al*.[91,92]	Glucose NIR 1,112–1,823 nm	Lip lining tissue and blood vessels	OGTT, calibration, prediction SEP = 3 mmol/L
Trans-reflectance of thumb	Gabriely *et al*.[15]	Glucose plus blood; 400–1,700 nm	SC, epidermis, dermis	Glucose clamp, calibration, SEP <0.28 mmol/L
Skin localized reflectance	Maruo *et al*.[95]	Glucose NIR 1,245–1,836 nm	Targets dermis layer	OGTT, calibration, prediction SEP = 1.45 mmol/L
Finger reflectance	Samann *et al*.[34]	Glucose NIR	SC, epidermis, dermis	Spot test, longitudinal calibration/prediction
Arm diffuse reflectance	Malin *et al*.[12]; Blank *et al*.[89]	Glucose NIR 1,050–2,450 nm	Epidermis and dermis	OGTT, calibration, prediction SEP = 1.39 mmol/L

ues than the NIR counterpart for *in vitro* whole-blood samples.

Heise and Marbach[21] used the ATR technique to characterize the outmost epidermal layer of human oral mucosa in the spectral range 800–4000 cm^{-1}. For several test subjects, lip spectra were recorded during an OGTT. The individually varying blood glucose concentration was followed by means of frequent blood testing. Oral mucosal spectra are supposed to vary with glucose concentration in the same way that aqueous solutions of glucose do. There was no evidence for an underlying glucose absorbance spectrum from analyzed data of this experiment. In another approach, difference spectra between the mean spectra of a subject with diabetes having a mean glucose value of 13.3 mmol/L and of a subject without diabetes having a mean value of 6.7 mmol/L showed a structured band (peak absorbance of 0.01 absorbance unit) in the 1,000 and 1,200 cm^{-1} range. Although there is no SC in the oral mucosa, the difference spectrum in this spectral interval resembles the published spectrum of the SC.[43,44] There was no clear evidence of mid-IR ATR sensing of changes in blood glucose concentration using this difference-spectra data analysis approach.[21]

Several patents by Berman and Roe[103–105] describe a method for the NI determination of glucose using mid-IR and an ATR element in touch with a human finger. Broadband IR energy is directed into the ATR element and subsequently into the skin. Spectra were recorded for the measurement range 1,000–1,053 cm^{-1} (10–9.5 μm) and for a reference range of 1,143–1,212 cm^{-1} (7.75–8.25 μm). The inventors realized that the light path does penetrate the SC layer only, and thus suggested that the skin compartment in which glucose is measured is the sweat glands or that glucose is transported from the sweat glands to the outer layer of the skin. The difference in the spectral signal, *S*, in the measurement range and the reference range is determined, and glucose concentration is deduced from a simple application of Beer's law. An empirical equation is used without the need for multivariate analysis:

$$[\text{Glucose, mg/dL}] = 1{,}950S - 17 \qquad (4)$$

Such simplicity is a welcome change to the NI glucose determination field, which is dominated by calculation-intensive methods.[21] Applying PLS regression to mid-IR ATR of the oral *S* value could not reliably relate the change in signal to changes in blood glucose concentration.[21]

Another aspect of the work of Berman and Roe[103–105] is that they applied a skin-cleansing step, prior to contacting the skin and the element. The steps involved in the cleaning are washing with water to remove surface glucose, washing with isopropanol to remove water, and then applying mineral oil to the skin. There are no mechanistic data as to what is the role of each of the washing steps or components on the optical properties of skin. This is important to understand, especially in light of the reported effect of isopropanol on the water content of the skin and on skin mid-IR ATR spectra.[45,46] Spectra published by Brancaleon *et al*.[46] show that the 1,000–1,100 cm^{-1} range of the spectra was affected both by the application of isopropanol and by tape-stripping of the SC.

Light scattering measurements

Measuring light scattering of tissues. NI determination of glucose was attempted using light scattering of tissue components measured by localized reflectance (spatially resolved diffuse reflectance) or NIR frequency domain reflectance techniques.[106–108] In localized reflectance measurements a narrow beam of light illuminates a restricted area on the surface of a body part, and reflected signals are measured at several distances from the illumination point. The values of μ_a and μ_s' for tissue can be deduced from the distribution of reflected light density as a function of source–detector (S-D) distances.[35] Both localized reflectance measurements and frequency domain measurements are based on change in glucose concentration, which affects the refractive index mismatch between the ISF and tissue fibers, and hence μ_s'.[20,106–108]

A glucose clamp experiment showed that $\delta\mu_s'$ at 650 nm qualitatively tracked changes blood glucose concentration for the volunteer with diabetes studied.[20] The distances between the source fibers and detector fibers (S-D dis-

tances) were in the range of 1–10 mm, which corresponds to the approximate depth in tissue upon which μ_s' is determined. In a second study, $\delta\mu_s'$ at 804 nm qualitatively tracked changes blood glucose concentration for the tested volunteers with diabetes. The S-D distances in this second study were in the range of 0.8–5.2 mm. Drift in μ_s' that was independent of glucose prevented statistical analysis and was attributed by the authors to other physiological processes contributing to $\delta\mu_s'$.[106] Changes in μ_s' did not exclusively result from changes in n_{medium} caused by increased glucose concentration. A third study using localized reflectance and OGTT involved five healthy volunteers and 13 volunteers with type 2 diabetes using two sensors placed on the abdomen.[107] The S-D distances in this study were in the range of 0.8–10 mm, and the wavelength at which the scattering coefficient was measured was 800 nm. In the case of the volunteers without diabetes 80% of measurements showed tracking between $\delta\mu_s'$ and blood glucose concentration. Twenty percent of measurements on those without diabetes showed no correlation between $\delta\mu_s'$ and blood glucose. Seventy-three percent of the localized reflectance measurements on those with diabetes resulted in a calibration models for μ_s' versus blood glucose concentration. In localized reflectance studies, the probe was continuously attached to the abdomen.[20,106,107] These studies did not address repositioning errors.

In a separate measurement in the same experiment a microdialysis probe was inserted in the abdominal tissue 10 cm away from the optical probe. Glucose concentrations in the ISF tracked blood glucose concentrations during the OGTT experiment, but lagged blood glucose values in stepwise clamp experiments. It was possible to establish a calibration model between $\delta\mu_s'$ and the concentrations of glucose in the ISF as determined by the microdialysis method.[107] The authors concluded that physiological changes in blood glucose could be monitored by determination of the $\delta\mu_s'$ in volunteers and patients with diabetes in most experiments.

The determined values of $\delta\mu_s'$ do not correlate with glucose concentration all the time. Glucose-independent drift in μ_s' has prevented statistical analysis. There was no attempt to study the cause of the inability to establish a calibration model when it happened. There are no new reported data on the NI determination of glucose using $\delta\mu_s'$ determined by frequency domain measurements.[108]

A possible interpretation for the poor correlation between measured $\delta\mu_s'$ and glucose concentration in the localized reflectance measurements with large S-D distances is that the depth in abdominal tissue spanned by light beams used in these measurements is ~10 mm. This depth encompasses the SC, epidermis, dermis, subcutaneous adipose tissue, and abdominal muscles. Bulow *et al*.[109] found that blood flow varied in the corresponding compartments in the human arm. Blood flow to the forearm and that to the subcutaneous tissue and skin in the forearm were measured by strain gauge plethysmography, ^{133}Xe-elimination flowmetry, and LDF, respectively, during an oral glucose load (1 g of glucose/kg of lean body mass) and during control experiments. Arterial glucose increased from 5.1 ± 0.3 to 7.8 ± 1.17 mmol/L at 30 min after initiating the glucose load, and decreased to 4.4 ± 1.17 mmol/L by the end of the experiment. The forearm blood flow remained constant during both glucose load and control experiments. Glucose induced a twofold vasodilatation in subcutaneous adipose tissue, which remained that way for the duration of the 240-min experiment. In skin, glucose induced a 50% relative increase in vasodilatation (over the aspartame control case) between 120 and 150 min. This tissue showed a relative vasoconstriction during the rest of the experiment. Muscle blood flow was estimated to decrease by about 20–30% during both glucose load and control experiments.

The vascular effect of glucose, and possibly the glucose concentration in tissue that is carried by the blood bolus, varies in the different tissue compartments. The optical signal will vary during the course of the glucose load (including glucose clamp, OGTT, or MTT) experiment. Although the data presented are for the forearm,[109] these arguments suggests that measurement of optical signal over multiple tissue compartments (layers) may contribute to the lack of quantitation in localized reflectance studies that use large S-D distances.[20,106,107]

A summary of the data on tissue scattering coefficient measurement of the abdomen is given in Table 3. No new data were reported using the frequency domain approach in the period covered by this review.

Measuring of light scattering by RBCs. An approach that is based on light scattering from RBCs was dubbed occlusion spectroscopy.[110–112] RBCs agglomerate in individuals with diabetes, especially upon occlusion, when the shear forces of blood flow are at a minimum. Finger blood vessels were occluded to slow blood flow and allow RBCs to aggregate. Change in light scattering upon occlusion was measured. Occlusion will not affect the rest of the tissue components, while scattering properties of agglomerated RBCs differ from those of the non-agglomerated ones and from the rest of the tissue.[110–112] It will thus be possible to separate scattering due to agglomerated RBCs from the scattering by the rest of the tissue components. The scattering coefficient of RBCs depends on the refractive index mismatch between the RBCs and blood plasma n_{RBC}/n_{plasma}, similar to the case of refractive index mismatch between connective tissue fibers and the ISF.[20,106–108] Change in glucose concentration affects n_{plasma}, and hence affects blood light scattering. Occlusion spectroscopy differs from that of localized reflectance and frequency domain measurements in that it proposes measurements of glucose in blood rather than in the ISF.[106–108]

The occlusion spectroscopy method was tested in a human study using a hyperinsulinemic-hypoglycemic clamp.[111] A linear calibration model was established with $R_c = 0.836$, but there were no reported error estimates. There was no reported interference from serum triglycerides, catecholamines, and cortisol, which were considered as potential interferents.[113] RBC aggregation is a complex phenomenon that is observed in the case of diabetes.[77] It has also been reported for other pathological conditions.[80–82] This raises the question of specificity. Other diseases affect RBC aggregation.[77–82] Clinical studies involving other molecular or cellular interferences and co-morbidities are needed to separate the effect of glucose on measured RBC scattering from other factors affecting shape and structure of RBCs. This technique addresses the compartmentalization issue and offers the potential of directly measuring the change in the refractive index of blood plasma, n_{plasma}.

Temperature-modulated localized reflectance measurement. Skin's thermo-optical response is sensitive to status of diabetes.[85] Blood glucose concentrations alter thermally modulated optical signals through physiologic and physical effects. Yeh *et al.*[11] studied the relation between skin thermo-optical response and blood glucose values. Temperature changes affect cutaneous vascular and refractive index responses, which in turn are affected by changes in glucose concentration.

Table 3. Tissue Scattering Coefficient Measurement Data on the Abdomen

Test type	*Reference*	*Optical system*	*Volunteers*	*Results*
Glucose clamp	Bruulsema *et al.*[106]	λ = 650 nm S-D distance 1–10 mm	With diabetes	Qualitative tracking of $\delta\mu_s'$ and glucose
Glucose clamp	Heinemann *et al.*[20]	λ = 804 nm S-D distance 0.8–5.2 mm	With diabetes	Qualitative tracking of $\delta\mu_s'$ and glucose in 73% of experiments
OGTT	Heinemann *et al.*[107]	λ = 800 nm S-D distance 0.8–10 mm	5 without diabetes	Calibration model in 80% of experiments with R_c >0.75, interexperiment and interperson bias, no prediction data
			13 with diabetes	Calibration model in 73% of experiments with R_c >0.75, interexperiment and interperson bias, no prediction data

A device based on the thermo-optical response of human skin was used to collect signal from the forearm of volunteers.[83–87] Glucose concentrations were correlated with temperature-modulated localized reflectance signals at wavelengths between 590 and 935 nm. There are no known NIR glucose absorption bands in this range. μ_a corresponds to blood absorption and thus reflects hemodynamic changes in cutaneous tissue. μ_s' is a measure of the refractive index mismatch between the ISF and tissue connective fibers.

Localized reflectance data were collected continuously over a 90-min period of probe–skin contact as temperature was repetitively stepped between 22°C and 38°C for 15 temperature modulation cycles. Each cycle comprised the following steps: Skin was equilibrated for 2 min at a probe temperature of 22°C, and the temperature was raised to 38°C over the course of 1 min, maintained for 2 min, and then lowered to 22°C over a 1-min period. At each temperature limit (during the 2-min window), four optical data packets were collected, and values of μ_a and μ_s' were determined. The method was tested in a series of experiments involving MTT and control runs. The control conditions were no-meal, cold water, or protein meals. Temperature modulation between 38°C and 22°C caused a periodic set of cutaneous refractive index and vascular changes, leading to periodic changes in skin reflectance.[11]

Yeh *et al.*[11] used a four-term LLS fitting of glucose to the reflectance data in the form:

$$[\text{Glucose}] = a_0 + \Sigma_i\, a_i \times R_i'\ (r,\lambda,T) \qquad (5)$$

The reflectance parameter $R'(r,\lambda,T)$, as defined by Eq. 5, equals $\log_e$ (measured localized reflectance). Thirty-two sequences of R' (at $T_{22°C}$) = $\log_e R(r,\lambda,T_{22°C})$ and R' (at $T_{38°C}$) = $\log_e R(r,\lambda,T_{38°C})$ were used in the LLS correlation. For each MTT over the 2-h period, the temperature sequences encompassed 20 data points.[11]

Changes in glucose concentrations were predicted using a model based on MTT calibration for each volunteer, with an SEP of <1.5 mmol/L and $R_p = 0.73$ in 80% of the experiments. There were run-to-run differences in the whole response curve of predicted glucose values in the form of an upward or downward shift of up to 5.6 mmol/L. These shifts were attributed to site-to-site structural differences.[11] Figure 2 shows an example of the MTT results for a volunteer with type 2 diabetes.

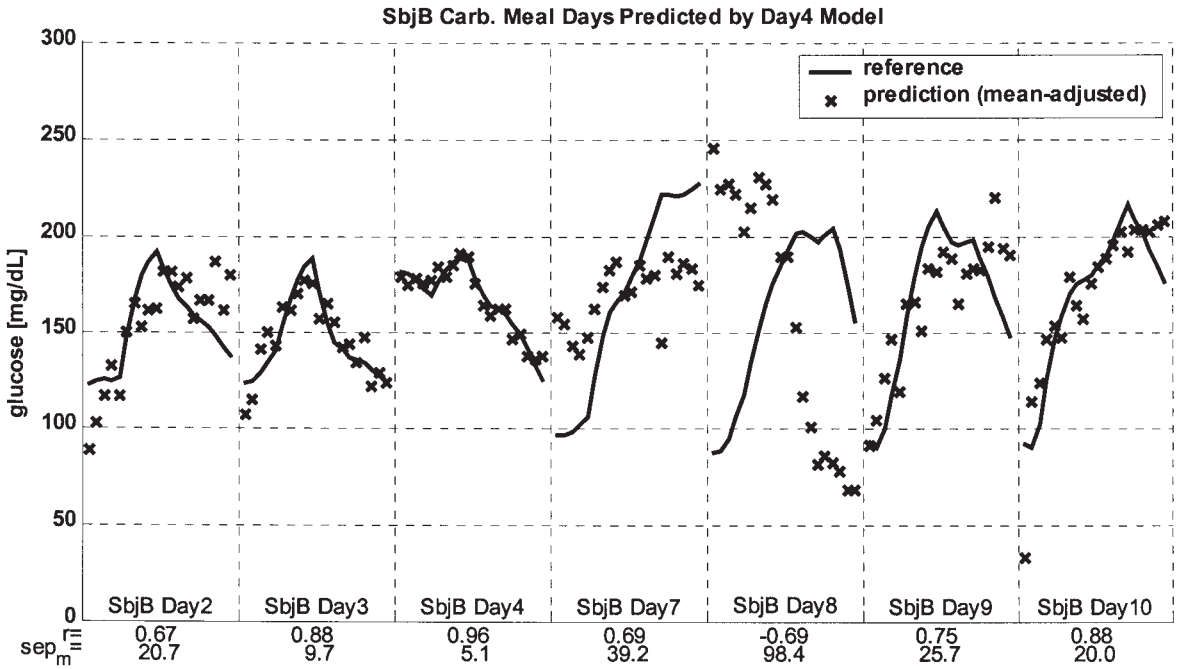

FIG. 2. Results of mean-adjusted prediction of glucose on an MMT on a volunteer subject (Sbj) with diabetes using the thermo-optical response of human skin. Day 4 was used for predicting the glucose concentration in other days. The individual response curves are mean-adjusted because of the day-to-day shift. Reproduced with permission of The American Association for Clinical Chemistry, from Yeh *et al.*[11]

The effect of temperature and change in glucose concentration on human skin are twofold: first affecting cutaneous vascular circulation (physiological effect) and second affecting cutaneous light scattering (physical effect). The correlation between glucose values and optical signals in this spectral range was attributed to the effect of glucose on the cutaneous hemodynamic response and on the refractive index.[11] Table 4 lists the mean-adjusted four-term LLS prediction parameters for MTT experiments on the two volunteers with diabetes.[11]

An MTT calibration model detected changes in glucose concentration in 80% of the MTT runs. The day-to-day shift in the response curve (bias in the signal) was attributed to probe positioning, cutaneous structural effects, or other physiological changes.[11] Maruo *et al*.[95] observed a similar bias in predicted glucose values in cutaneous NIR absorption experiment.

There was a fortuitous observation for volunteer B on run #8 in Table 4; the subject had fever due to influenza infection. The R_p value for run #8 was negative ($R_p = -0.69$), and the SEP was >5.5 mmol/L. Experiments on this volunteer were repeated later as tabulated at the bottom of Table 4.[11] The effect of fever in this case suggests that testing an NI glucose detection method should be performed under different disease conditions, in addition to diabetes.

Glucose concentrations in control runs (noncarbohydrate meals) showed considerable scatter when predicted by an MTT calibration model. The calculated SEP was higher than the measured glucose range in cases where the glucose range was <2 mmol/L. SEP values up to 2.74 mmol/L were calculated for a protein meal experiment where there was no change in glucose concentration. This raised the question of what can be used as a control experiment for NI measurements. For the case of protein meal runs, cutaneous hemodynamic changes due to digestion affected the optical signal. The extent, rate, and direction of cutaneous hemodynamic response to protein meals may be different from those caused by the change in glucose concentration. Further work is needed to test this method in a spot test experiment.

The thermo-optical response method offers certain compartmentalization advantages over localized reflectance measurements that use large S-D distances,[20,106–108] as it limits sampling depth to the dermis by virtue of the probe design (short S-D distances) and the use of temperature control. The detection method incorporates temperature effect on both NIR absorption and scattering processes. No glucose specificity advantage has been established yet over of the use of μ_s' determined by frequency domain or spatially resolved measurements.[106–108]

Optical coherence tomography (OCT). OCT is a tissue imaging technique that allows depth resolution of less than 10 μm.[114,115] It allows determination of refractive index and scattering coefficient values in layered structures in skin, *e.g.*, SC, epidermis, and dermis. The apparatus consists of a low coherence light source such as

Table 4. Mean-Adjusted Four-Term LLS Prediction Parameters for Carbohydrate-Meal Experiments

	Volunteer A			*Volunteer B*		
Day	*Glucose range (mmol/L)*	*Mean-adjusted* R_p	*Mean-adjusted SEP (mmol/L)*	*Glucose range (mmol/L)*	*Mean-adjusted* R_p	*Mean-adjusted SEP (mmol/L)*
2	6.93	0.84	1.51	3.84	0.67	1.15
3	6.67	[a]	[a]	3.62	0.88	0.54
4	6.3	0.86	1.17	3.49	[a]	[a]
7	7.04	0.94	0.96	7.27	0.69	2.18
8	4.45	0.73	1.10	6.46	−0.69	5.46
9	7.22	0.85	1.34	6.84	0.75	1.43
Repeat of day 8	—	—	—	7.03	0.88	1.11

Reproduced with permission of The American Association for Clinical Chemistry, from Yeh *et al*.[11]
[a]Data set used as a calibration model.

a superluminescent diode and an interferometer, which determines the depth of the backscattering feature by measuring the delay correlation between backscattered light in the sample and the reflected light in the interferometer arm. OCT of the palm of the hand and the volar side of the arm (wavelength) showed a decrease in the refractive index of the SC, a drop in the μ_s' of the epidermis, and a rise in μ_s' of the SC over the 1–1.5-h period. The behavior of the SC was interpreted by moisture uptake from sweating.[116,117] The effect of moisture uptake and sweating as a result of interaction of measuring probe with skin and their contributions to signal variations has not been estimated.

OCT was proposed for the NI detection of glucose with no experimental data presented.[118] The technique was applied afresh to NI determination of glucose by scanning a two-dimensional image of the skin and then converting it to a single curve to obtain a one-dimensional distribution of light intensity as a function of depth. The experimental set up is shown in Figure 3. The slope of the OCT signal versus depth line is determined and is correlated with the concentration of blood glucose.[119–122] An example of the output of the detection method is shown in Figure 4. First an image of the layers of skin determined by OCT is shown in Figure 4A. In the bottom part the OCT signal as a function of depth is shown. The various skin layers are indicated in Arabic numerals. The slope of the portion of the plot in the dermis layer is used to calculate μ_s'. In an anesthetized animal skin experiment, OCT images at 1,300 nm illumination wavelength demonstrate that glucose affects the refractive index mismatch in skin and decreases μ_s'.[121] The effect of glucose on the μ_s' values measured by OCT was similar to the effect measured by localized reflectance or frequency domain measurements.[20,106–108]

The stability of the slope of the OCT signal was dependent on tissue heterogeneity and motion artifacts. Moderate skin temperature fluctuations (±1°C) did not decrease accuracy, but substantial change (± several degrees Celsius) significantly affected the OCT signal slope, *i.e.*, μ_s', an effect that is similar to that observed in the thermo-optical response studies of human skin.[11]

An OCT system with a light source of 1,300 nm was used to test 15 healthy volunteers in 18 OGTT clinical experiments. OCT images were taken every 10–20 s from the left forearm over a total period of 3 h. Venous blood was sampled from the right arm vein every 5 or 15 min. The slope of the OCT signals versus depth was calculated for a depth of 200–600 μm below skin surface. Figure 5A shows OCT signal tracking of changes in glucose concentration. The OCT signal change is plotted in the reverse direction. The slope of OCT signals correlated with blood glucose concentrations throughout the duration of the experiments as is shown in Figure 5B, changing up to 2.8% per mmol/L of plasma glucose values.[119,122]

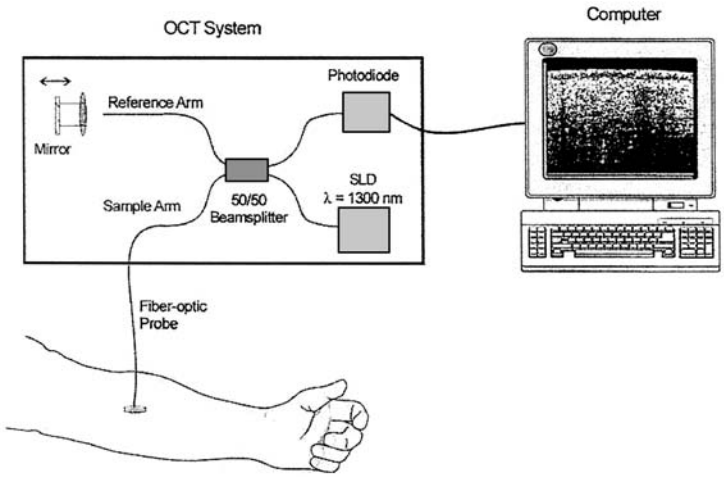

FIG. 3. Optical layout of the OCT system. Light from the 1,300 nm superluminescent diode (SLD) is split between the reference and sample arms of the interferometer. Depth measurement is achieved by moving the mirror with respect to the reference arm. Reproduced with permission of the American Diabetes Association, from Larin *et al.*[119]

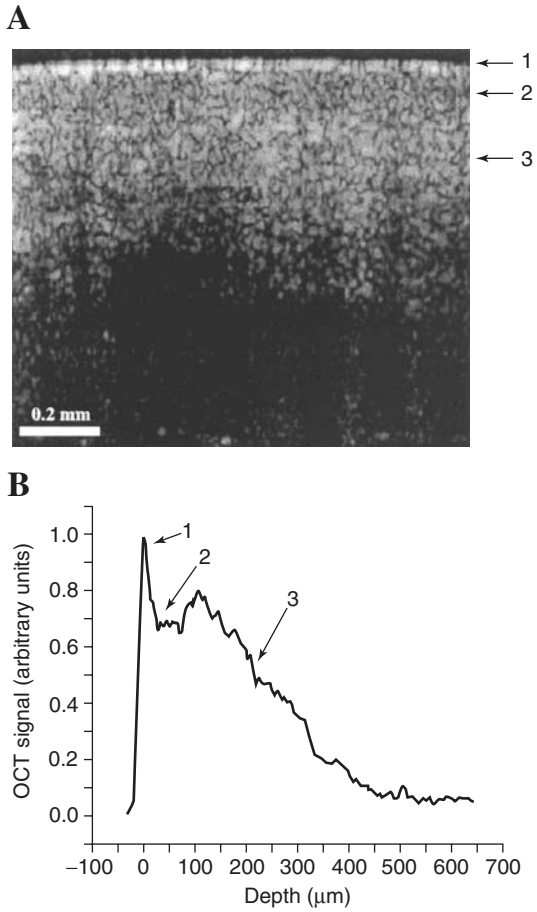

FIG. 4. **A:** Typical OCT image obtained from skin of a volunteer using 1,300 nm excitation. **B:** Corresponding one-dimensional OCT signal. The numbers on the graph refer to the different cutaneous layers: (1) SC; (2) epidermis layer; and (3) dermis. The slope of the OCT signal versus depth is close to linear in the dermis layer and is related to the scattering coefficient. It was used for correlation with glucose concentration. Reproduced with permission of the American Diabetes Association, from Larin *et al*.[119]

The OCT technique is promising as the optical measurements targets a restricted area in the skin. Unlike the localized reflectance method that uses large S-D distances and spans multiple layers in tissues,[20,106–108] OCT addresses the issue of skin layers. It offers certain compartmentalization advantages over localized reflectance measurements, as it limits sampling depth to the upper dermis without unwanted signal from other layers. OCT measurement has been attempted only in an OGTT or clamp-like studies where there is a sequential rise and fall of glucose concentration. It has not been attempted in spot-testing situations or in longitudinal studies. Like other scattering techniques, the detected phenomenon is the effect of glucose on the refractive index of the ISF. It does not address the effect of circulation and temperature changes. No specificity advantage has been established for OCT over other scattering studies.[106–108]

A summary of the human data of methods based on light scattering measurements is shown in Table 5. Localized reflectance on human abdomen spans different tissue compartments down to 10 mm.[106–108] These include the

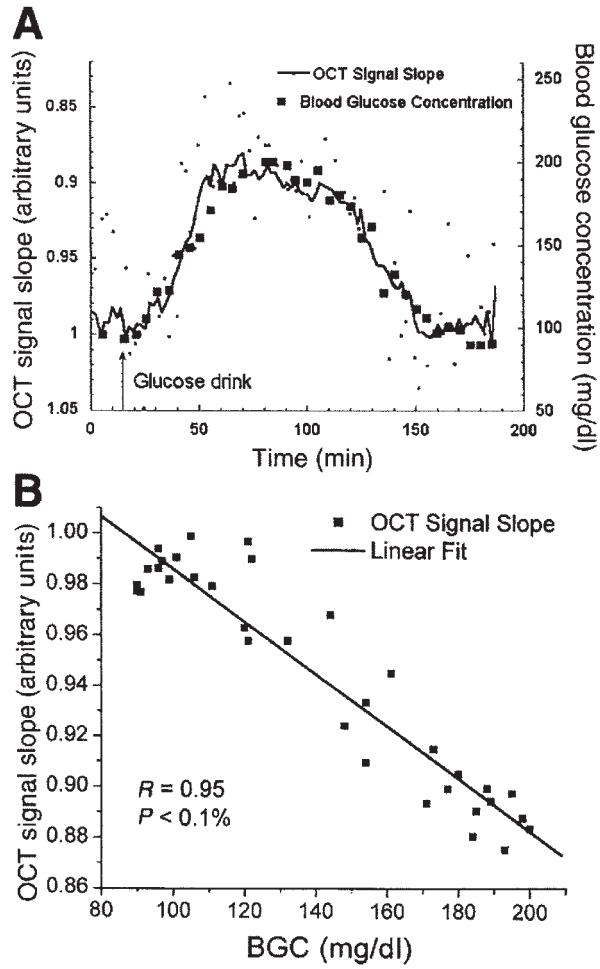

FIG. 5. **A:** Slope of OCT signals (plotted in the inverted scale) and corresponding blood glucose concentrations obtained from a volunteer without diabetes. The blood glucose concentration was measured every 5 min. Dots represent the OCT signal slope (in arbitrary units), and the black line represents the fit of the data points. The black small squares are the invasively measured blood glucose concentrations. **B:** Slope of OCT signals versus blood glucose concentration (BGC) for the data shown in A. *R*, correlation coefficient. Dots represent the OCT signal slope, and the line represents the linear fit of the OCT data points. Reproduced with permission of the American Diabetes Association, from Larin *et al*.[119]

Table 5. Human Data on Methods Based on Light Scattering Measurements

Method		*Specificity*	*Compartmentalization*	*Calibration*
Localized reflectance of abdomen	Heinemann *et al.*[20]; Bruulsema *et al.*[106]	Glucose effect on n_{ISF}	Dermis, subcutaneous fat, and muscles 0.8–10 mm depth, abdomen	Glucose clamp or OGTT, calibration model
Thermo-optical response	Yeh *et al.*[11]	Glucose effect on n_{ISF} and perfusion	Dermis 0.4 to <2 mm depth, forearm	OGTT, calibration model/prediction
RBC scattering	Shvartsman and Fine[110]; Cohen *et al.*[111]	Glucose effect on n_{plasma}	Blood vessels	Clamp, calibration model
OCT	Larin *et al.*[119,121,122]; Esenaliev *et al.*[120]	Glucose effect on n_{ISF}	Upper dermis 200–600 μm depth, forearm	OGTT, calibration model

dermis, subcutaneous fat, muscles, and blood vessels therein. OCT localized μ_s' measurements to the dermis, RBC scattering localized it to cutaneous blood vessels, and temperature modulation studies localized scattering and perfusion measurements to the dermis.

Optical activity and polarimetry

Polarimetry has been used for quantitative analysis of solutions of optically active (chiral) compounds such as glucose. When a beam of plane-polarized light transverses a solution, its plane of polarization rotates by an angle α, which is related to the concentration of the optically active solute. Optical rotation in the eye was the earliest proposed NI methods for NI determination of glucose.[123] Several advances in the polarimetry technique have been reported. Rawer *et al.*[124] discussed different approaches to utilizing the polarizing properties of the aqueous humor (AH) for quantitative glucose measurements. Cameron *et al.*[125] presented *in vivo* results from a laser-based optical polarimetry system using the anterior chamber of a rabbit eye. The time delay between blood glucose and NI-measured glucose in AH was reported to be less than 5 min in rabbit eye.[126] In a different study AH glucose in a rabbit's eyeball lagged blood glucose values by a 30-min delay.[127] Lane *et al.*[128] studied the acute effect of insulin on AH. Under euglycemic conditions of high and relatively low insulin concentrations, AH flow through the anterior segment of the eye decreased in patients with type 1 diabetes.[128] Bockle *et al.*[129] described a new Brewster-angle approach to determination of change in degree of polarization. Polarimetry requires a body part with low scattering such as cornea, appropriate calibration, and understanding of lag time between blood glucose and AH glucose. The eye offers an advantage over the skin for NI measurements of glucose because of the absence of the SC. Corneal rotation, corneal birefringence, and eye motion artifact are potential source of error in polarimetric ocular measurements.[1]

Raman scattering

Use of Raman spectroscopy for the detection of glucose falls in the category of methods that measure an intrinsic property of the glucose molecule. Most recent Raman studies are *in vitro* measurements. Raman bands at 900–1,200 cm^{-1} are specific to the molecular structure of glucose.[130,131] Fundamental vibrations monitored by Raman spectroscopy are sharper and have less overlap compared with NIR combination bands. Additionally, water has a low Raman cross section. The advent of NIR Raman spectrometers and use of multivariate spectral analysis for extracting diagnostic, chemical, and morphological information extended the application of Raman spectroscopy to various clinical applications.[130,131]

Raman spectra of blood samples excited at 830 nm yielded an SEP of 3.6 mmol/L glucose.[132] Feld's group developed a method of linear multivariate calibration called hybrid linear analysis (HLA),[133] which involves incorporating the spectrum of the desired species (glucose) into the calibration procedure. The SEP for glucose in serum obtained with PLS is 1.2 mmol/L, and the SEP obtained with HLA is 0.94 mmol/L. In whole blood, the PLS-SEP for glucose was 4.4 mmol/L, and the HLA-determined SEP was 3.5 mmol/L.[134] The calibration model was stable over a 7-week period. SEP increased on going from serum to whole blood.

Raman spectra of the AH of the eyes from 32 anesthetized rabbits that were excited at 785 nm and corrected to eliminate broadband fluorescence showed fair correlation with glucose concentration ($R_c = 0.87$).[135] Correlation improved when fluorescence was subtracted prior to linear multivariate analysis ($R_c = 0.95$). Adding an artificial neural network to the analysis further improved the correlation ($R_c = 0.99$). AH glucose exceeded blood glucose values at normoglycemic levels. It correlated linearly with plasma glucose above 11 mmol/L.

Raman measurements on intact human skin are expected to be more complex than the case of solutions or of blood. Raman spectral images of skin showed some complex lipid structures.[136] Chaiken *et al.*[137,138] studied Raman spectra of human skin under tissue modulation conditions, which involved the use of thermal and/or mechanical stimuli to produce distributions of blood-rich "replete" and blood-deficient "deplete" regions of skin. Raman spectra of human blood *in vivo* were excited at 785 nm or 830 nm, and the corrected integrated normalized intensities of the Raman shifted bands between 400 and 1,800 cm^{-1} were calculated. Blood volume variations and fluorescence corrections were used to improve signal quality.[138] Human data that were obtained at 905 nm excitation showed that the corrected integrated signal could be fitted to the capillary glucose values for 23 individuals with $R_c = 0.74$. Repeated measurements on three individuals with a total of 28 data points yielded $R_c = 0.63$. Fitting the Raman signal to glucose concentration separately for each of five individuals yielded $R_c > 0.9$ for the single-person calibration.

Surface-enhanced Raman scattering (SERS) is an effect that results in enhancing the intensity of Raman bands of molecules localized in close proximity of silver and gold surfaces. Raman scattering intensity increases when a molecule is spatially confined within the range of the electromagnetic fields generated upon excitations of the localized plasmon resonance of nanostructured silver or gold surface. Several orders of magnitude of sensitivity enhancement can be gained over conventional Raman spectroscopy,[139] which may shorten the data acquisition time. Molecules confined within a decay length of the plasmon electromagnetic field of 0–4 nm will exhibit SERS spectra even if they are not chemisorbed.[140]

In a recent report, glucose was partitioned into an alkanethiol monolayer adsorbed on a silver film over nanospheres (AgFON).[141] PLS calculations demonstrated the ability to establish a calibration model for SERS signal versus glucose concentration. The model was validated by LOOCV over a 0–25 mmol/L concentration range with an SECV of 1.8 mmol/L.[141] Enhancement in the Raman signal is important for both minimally invasive and NI glucose determination. The partition layer was changed to alkane thiolate tri(ethylene glycol) monolayers in order to increase its stability.[142] The partition rates improved, and the sensor stability increased. The SECV of glucose in water was 1.8 mmol/L, and 4.56 mmol/L in the presence of albumin.[142] The rate of improvement in this technology makes it a promising sensor at least for minimally invasive sensing in the ISF.

PA spectroscopy

PA spectroscopy is used to detect weak absorbencies in liquids and gases.[143] A PA measurement is an alternative detection technology for light interaction with tissues.[144–148] The medium is excited by a picosecond to nanosecond laser pulse at a wavelength that is absorbed by a particular molecular species in the medium. Light absorption and subsequent radiationless decay cause microscopic localized heating in the medium, which generates an ultrasound pressure wave that is detectable by a

hydrophone or a piezoelectric device. The pulsed PA signal is related to the properties of a clear medium by the equation:

$$\mathrm{PA} = k(\beta v^n / C_\mathrm{p}) E_0 \mu_\mathrm{a} \quad (6)$$

where PA is the signal amplitude, k is a proportionality constant, E_0 is the incident pulse energy, β is the thermal expansion coefficient, v is the speed of sound in the medium, $n = 2$, C_p is the specific heat, and μ_a is the light absorption coefficient. This equation applies to clear solutions or crystals.

PA spectroscopy is relatively unaffected by scattering in optically thin (clear) media, but is affected by scattering in optically dense media. Light scattering in the medium affects the shape of the PA pulse. In highly scattering media μ_eff replaced μ_a. Dispersion of the PA signal as a function of wavelength mimics the absorption spectrum in optically thin (clear) medium. It is equivalent to the diffuse reflectance spectrum in an optically dense medium. Fainchtein *et al*.[145] provided detailed analysis of generation and propagation of PA signals in blood.

MacKenzie *et al*.[144] studied the PA effect in glucose solution in the low scattering case. PA signal generation is assumed to be due to initial light absorption by the glucose molecules. Solutions were excited by NIR laser pulses in the 1,000–1,800 nm range, at wavelengths that corresponded to NIR absorption of glucose. There was a linear relationship between PA signal and glucose concentration in aqueous solutions.[144] Human experiments showed that the PA signal tracks change in glucose concentration.[144] No data analysis was presented to show an advantage of PA spectroscopy over an NIR transmission or reflectance for NI measurement of glucose.

A different approach is the use of ultraviolet laser pulses at 355 nm. The generated pulsed PA time profile is used to detect the effect of glucose on tissue scattering, which is reduced by increasing glucose concentration.[146] PA time profiles were analyzed to yield μ_eff, which like μ_s' is related to changes in the refractive index of the medium induced by changes in glucose concentration. *In vivo* PA profiles measured in rabbit sclera before and after intravenous glucose administering demonstrated that a 1 mmol/L increase in glucose concentration resulted in a 3% decrease of μ_eff. In this case the absorbing species is one of the amino acid residues in the sclera, and the PA pulse shape is modulated by light scattering expressed by μ_s', which is dependent on the concentration of glucose through its effect on the refractive index. Additionally, the thermoelastic parameters of the medium β,v, and C_p also affect the magnitude of the signal in a way that is related to glucose concentration.

Absorption of laser pulses by the glucose molecules is not the only mechanism necessary for observation of the PA effect. From Eq. 6, once a compression wave is generated after light absorption by any chromophore in the medium, the resultant PA pulse intensity can be modified by the medium thermoelastic properties β,v, and C_p. All three properties are dependent on glucose concentration. Using the equation $P = k(\beta v^n / C_\mathrm{p}) E_0 \mu_\mathrm{a}$ to analyze the data presented in the dissertation by Zhao[148] shows that in response to a 1% change in glucose concentration in water solutions, the calculated thermal expansion coefficient β, specific heat C_p, and acoustic velocity v changed by 1.2%, −0.6%, and 0.28%, respectively. By including the three parameters in the equation, the calculated change in the amplitude of the PA signal is 2.05%. The measured change in the acoustic signal, at 905 nm excitation, was 2%. Thus it is possible to account for the magnitude of the PA signal excited at 905 nm without taking into consideration the absorption coefficient of glucose. The optical absorption coefficient at 905 nm is 0.007 mm^{-1}. At this wavelength the optical absorption by glucose contributes negligibly to the signal.[148]

Addition of a scattering component to the medium enhanced the PA signal exited at 905 nm. The PA signal resulting from 55.56 mmol/L (1 g/dL) glucose increased by 250% in 3% milk solution, by 50% in tissue, and by 700% in blood as compared with its magnitude in clear water solutions.[147,148] Temporal dispersion PA curves of blood suspensions containing glucose and excited by a 905 nm pulsed laser source demonstrated that glucose decreased μ_s'.[147,148] This effect is similar to the PA signals from the eye sclera.[146] It is also similar

to the scattering μ_s' on tissue and turbid media.[106,119,122] The absorbing species at 905 nm is most probably the hemoglobin molecule. The parameter measured by the PA effect in blood suspensions at 905 nm is most probably the effective attenuation coefficient μ_{eff}.

The interplay of light absorption and medium properties change on the PA signal was further investigated by Shen *et al.*,[149] who determined time profiles of pulsed PA signals in graphite suspensions at excited at 900 nm. The suspensions had absorbance values ranging between 12 to 53 absorbance units/cm. The PA-determined μ_a, using Eq. 6, was linearly related to absorbance measured by an NIR spectrophotometer. PA signals for glucose in water were measured at 1,450 nm with concentrations ranging between 111 and 833 mmol/L. The behavior of the signal change was indicative of the water displacement effect. The PA signal reached the detector faster at higher glucose concentrations. The data were interpreted as meaning that in the graphite case, the dominant effect was the absorption coefficient in Eq. 6. In the glucose case at 1,450 nm excitation, it was the effect of glucose on the sound velocity in the medium.[149] The direction of signal change was similar to that of water displacement in the NIR absorption at 1,450 nm. The concentration and optical densities used were much higher than the physiological glucose concentration or tissue light absorption ranges.

Measurement of sound propagation in tissue is dependent on mechanical coupling between the skin and the measuring probe and the pressure of the probe on the skin. This effect is quite similar to ultrasound propagation in tissue where coupling jells are used to improve the speed of sound matching and decrease sound reflections. Dependence of the signal on probe–skin interaction is obvious in NIR optical methods.

Still further work is needed to understand PA origination and propagation in tissue and its use for NI determination of glucose. The PA effect was not shown to offer any advantages in detection specificity over other NIR absorption or diffuse reflectance methods. It is possible to account for the measured magnitude of the signal under some experimental conditions by factors other than the NIR absorption of glucose. The enhancement of the signal in blood that was excited at 905 nm is probably due to light absorption by hemoglobin and modification of the signal by glucose.[147,148] In the scattering mode, PA does not offer any noticeable advantage over other scattering methods. The PA signal tracks μ_{eff} in scattering media. The pulse profile is related to the μ_s' and is dependent on the refractive index mismatch between scattering centers and the medium.[146] The nature of absorptive events or the "absorbing chromophore" that generates the PA signal is not known with certainty. There is no evidence that glucose molecules are the primary absorbing species of the NIR light pulse that generates the compression wave. Water, glucose, blood, and tissue amino acid residues can absorb NIR light pulses. The generated compression wave is modulated by scattering and thermoelastic properties of the medium, which change with change in glucose concentrations.

Glucon, Inc. presented a novel PA application in the Diabetes Technology Meeting in Atlanta in November 2002, which is posted on their web site.[150] Additionally, several variations on combining ultrasound and PA spectroscopy were described in a patent publication.[151] The methods presented include:

1. Use of an ultrasound transducer to locate a bolus of blood in a vessel and then illuminate it with a pulsed laser at a glucose absorption wavelength. The same ultrasound transducer detects the generated PA signal.
2. A second variation is to detect ultrasound signal reflected from a blood vessel before and after PA excitation. Glucose is then determined from the difference in reflected ultrasound intensity.
3. A third approach is to excite a blood bolus in a vessel via a PA effect. The change in the dimensions and speed of the excited bolus causes a Doppler shift to an ultrasound pulse directed towards the blood vessel. Glucose is determined from the magnitude and the delay of the Doppler-shifted ultrasound peak.[150,151]

The purpose of combining of ultrasound and PA is to target a specific body compartment, mainly a blood vessel, thus addressing the

compartmentalization issue. Specificity needs to be addressed. Is the PA signal due to specific glucose absorption or due to blood component absorption of the pulse, and then glucose affects the plasma thermoelastic and refractive properties? There are no published clinical data, but it is posted on the Glucon, Inc. web site.[150] Human data on pulsed PA determination of glucose are given in Table 6.

PA is emerging as a novel blood vessel imaging modality and may be useful to study diabetes vascular complications. Hoelen *et al*.[152] imaged blood vessels in highly scattering samples, using 532 nm light, to depths of ~1 cm.

Thermal and IR emission measurements

Thermal gradient spectroscopy (TGS), an IR emission technique, is based on measuring the fundamental absorption bands of glucose at 9.1–10.5 μm, and bands of other analytes such as water and proteins. A prototype incorporating the technology has been described.[153–156] In TGS technology the spectroscopic energy source is the body's naturally emitted IR energy, which is absorbed by glucose at ~10 μm.

In one application of TGS the surface of the skin is cooled to approximately 10°C to suppress its absorptive effect. NIR light penetration depth in skin increased by lowering its temperature, which can help targeting a particular cutaneous layer.[85–87] This is attributed to a decrease in absorption and scattering coefficients. The cooling-induced skin transparency allows monitoring of IR emission from the ISF and cutaneous layers.[153–156] Using IR emission instead of IR absorption allows sampling of deeper cutaneous layers below the SC, which is the layer sampled by mid-IR absorption measurements. *In vivo* clinical data on several individuals with type 1 diabetes have been reported.[153] A linear response between *in vivo* detected glucose and reference blood glucose values has been reported. Multiple LLS fitting to the calibration data yielded an SD of 1.4 mmol/L.

In an alternate application of TGS[155,156] the skin surface is continually cycled up and down in temperature ±5°C around normal skin surface temperature at a rate of approximately 1 Hz. The resulting thermal oscillation produces a modulated IR signal, which is dispersed into selected mid-IR bands by IR-pass filters, detected, and synchronously demodulated. In this technique the relative phase of the signal at each wavelength relates directly to the relative spectral absorption of the tissue at each mid-IR wavelength. An algorithm transforms this phase difference into a mid-IR absorption spectrum. Once the mid-IR absorption spectrum has been determined conventional spectroscopic techniques are proposed to be employed to quantify glucose. TGS offers specificity and compartmentalization advantages. LLS fitting was used, but the fitting conditions and the proprietary transformation algorithm were not disclosed in sufficient details.

Measurement of the amplitude of IR emission from the tympanic membrane using a fil-

Table 6. Summary of Pulsed PA Determination of Glucose

Method	*Reference*	*Specificity*	*Compartmentalization*	*Calibration*
PA absorption, >1,500 nm	MacKenzie *et al*.[144]	Glucose absorption	Finger tissue and vessels	OGTT, calibration model, SEP not reported
PA scattering, 355 nm	Bednov *et al*.[146]	Glucose effect on $n_{\text{vitreous fluid}}$	Eye	Animal model, calibration model, SEP not reported
PA scattering, 905 nm	Zhao[148]	Glucose effect on n_{ISF}	Dermal tissue, forearm	OGTT, calibration model, SEP not reported
PA/ultrasound, 700–900 nm	Glucon[150]; Nagar *et al*.[151]	Glucose effect on n_{ISF}	Blood vessels, forearm	OGTT, calibration model, SEP not reported

ter at 10.5 μm and signal difference to a known glucose concentration has been proposed. The data indicate tracking between the signal and glucose concentration in an MTT.[157,158] Buchert[157] suggested a method that is based on the premises that the human body naturally emits IR energy, a portion of which is characteristic of glucose and can be utilized for its NI determination. The method utilized a sensor inserted in the ear canal to measure IR radiation emitted by the tympanic membrane. Ear thermometers are commonly used to measure body temperature from the wavelength-integrated intensity of IR radiation emitted from the tympanic membrane. The tympanic membrane is an excellent site to measure body temperature because it shares its blood supply with the hypothalamus, the center of core body temperature regulation. When compared with the theoretical blackbody radiation this IR radiation of the tympanic membrane is spectrally modified by blood glucose, which changes the membrane's emissivity and make it possible to measure the concentration of blood glucose.[157,158]

Malchoff *et al*.[158] described an NI glucose monitoring test device that is schematically shown in Figure 6. The instrument, which detects IR radiation from the tympanic membrane, consists of two thermopile detector/optical IR filter sets. One of the sensing elements is covered by a 9.6-μm IR filter sensitive to a glucose IR wavelength. The second sensing element is covered with a filter that does not have spectral bands of glucose such as the quasi-isosbestic point at about 8.5 μm. Spectrally modified IR radiation from the tympanic membrane illuminates both detectors. The difference in radiation intensity between the two radiation paths provides a measure proportional to glucose concentration.[157]

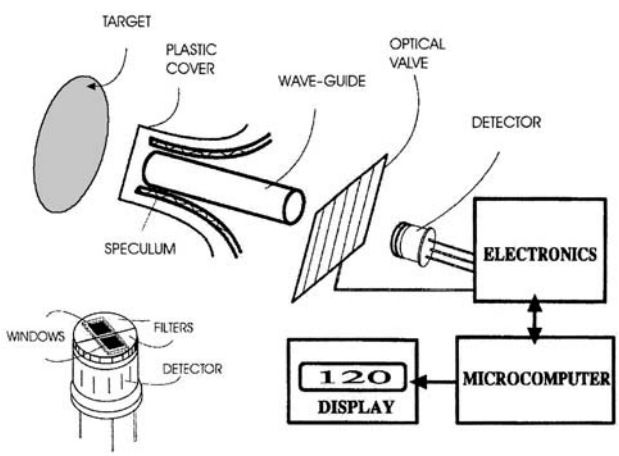

FIG. 6. Schematic of the IR emission detection of glucose. The target is the tympanic membrane; the waveguide, inserted in the ear canal, directs the IR radiation to the light valve and then to the detector. Reproduced with permission of the American Diabetes Association, from Malchoff *et al*.[158]

IR emission from the tympanic membrane was calibrated versus serum glucose concentration using 432 paired measurements from 20 subjects with insulin-dependent diabetes. The calibration was subsequently tested in a blind fashion with 126 paired measurements from six volunteers with diabetes.[158] Based on the calibration model, predicted glucose concentrations had an SD of 1.48 mmol/L, with R_p = 0.87. Data presentation differs from used for most multivariate methods. It is not clear whether this SD is equivalent to SECV or SEP.

The simplicity of this method and the acceptance of the ear thermometers make it quite appealing. Overlap between the effect of glucose on the signal and temperature variations due to circadian periodicity needs to be delineated. There is a need to separate the measurement technique as a temperature response to glucose change, blood flow response to glucose change, or an intrinsic glucose property (IR emission from the glucose molecule). Probably a "fever effect" such as shown in other correlations should be explored.[11]

Fluorescence measurements

Skin fluoresces at 370 and 455 nm when it is excited by ultraviolet light. Multiple regression analysis shows correlations between skin autofluorescence and pigmentation (melanin), redness (hemoglobin), and epidermal thickness. Skin autofluorescence depended on pigmentation, redness, and epidermal thickness, in a descending order.[159] Snyder and Grundfest[160] patented the use of laser-induced fluorescence for the NI determination of glucose. When glucose solutions were excited with an excimer laser line at 308 nm, fluorescence was detected at 340 and 400 nm, with fluorescence maximum at 380 nm.[160] Fluorescence intensity changed with change in glucose concentration

in an aqueous medium. Glucose does not have electronic absorption bands in this short ultraviolet spectral range. The patent does not explain the molecular origin of this fluorescence. Exciting the skin at this short wavelength will lead to a strong scattering component, in addition to the fluorescence. There are no available human data on NI glucose determination by direct ultraviolet excitation of human tissue.

In vitro fluorescence assays for glucose have been studied as steps towards its *in vivo* determination. Several methods are based on fluorescent resonance energy transfer (FRET) and on competition between glucose and dextran for concanavalin-A (con-A) binding sites. The assay components are con-A labeled with an energy acceptor, or an energy donor, and dextran labeled with the complementary molecule for FRET.[161–163]

A fluorescence biosensor incorporates rhodamine-labeled con-A [tetramethylrhodamine isothiocyanate (TRITC)-con-A)] as the energy acceptor and fluorescein isothiocyanate-dextran (FITC-dextran) as the energy donor. Both molecules are chemically conjugated into a hydrogel network.[161] In the absence of glucose, TRITC-con-A binds with FITC-dextran, and the FITC fluorescence is quenched through FRET. Competitive glucose binding to TRITC-con-A liberates FITC-dextran, resulting in increased fluorescence intensity proportional to the glucose concentration. The *in vitro* fluorescence response was linear over a glucose range between 0 and 33 mmol/L.[161] Another glucose assay uses FRET between con-A labeled with fluorescent protein allophycocyanin as donor, and dextran-malachite green as an energy acceptor. Glucose competitively displaces dextran-malachite green and increases allophycocyanin fluorescence intensity. The *in vitro* assay had a glucose dynamic range of 2.5–30 mmol/L.[162,163]

Evans *et al*.[164] developed an *in vitro* cell culture model of skin-component cells as a model to test the NI glucose monitoring by measuring NAD(P)H-related fluorescence changes in tissues. NAD(P)H solutions fluoresce at 400–500 nm when excited at 340 nm. 3T3-L1 fibroblasts and adipocytes were grown in culture, and the response to added glucose was assessed by changes in steady-state autofluorescence at 400–500 nm.[164] Spectral properties indicated that the fluorescence was due to NAD(P)H production. Cells stained with the fluorescent mitochondrial marker rhodamine-123 showed immediate and marked decrease in fluorescence when exposed to glucose.[164]

Masters *et al*.[165] demonstrated the use of multiphoton excitation fluorescence microscopy (MPFM) for functional imaging of the metabolic states of *in vivo* human skin cells. MPFM at 730 and 960 nm was used to image *in vivo* human skin autofluorescence from the surface to a depth of approximately 200 μm. Fluorescence lifetime images were obtained at selected locations near the surface (0–50 μm) and at deeper depths (100–150 μm) for both excitation wavelengths. Cell borders and cell nuclei were the prominent structures observed. NAD(P)H was found to be the primary source of the skin autofluorescence for the 730 nm two-photon excitation. A two-photon fluorescence emission at 520 nm was attributed to flavoprotein.[165] NAD(P)H is involved in glucose metabolism. Change in NAD(P)H fluorescence in adipocytes, keratinocytes, and other upper dermis components, when measured by MPFM, may be used to track glucose changes in human skin. Spectroscopic methods to decrease or diminish the effect of skin scattering can be used to improve the quality of fluorescence signals. The effects of other compounds that utilize the NAD(P)H in their metabolic pathways need to be investigated.

Measurement of skin fluorescence from the epidermis, or the upper dermis, will require the use of confocal fluorescence microscopy.[166] Swindle *et al*.[167] reported the ability of *in vivo* fluorescence point-scanning laser confocal microscopy to produce real-time, high-resolution images of the microscopic architecture of normal human epidermis using an NI imaging technology.

March and co-workers polymerized a fluorescent complex within a hydrogel to make an intraocular lens that responds well to glucose concentration.[168,169] The patient wears the lens, which changes its fluorescence depending on glucose concentration. Fluorescence is excited and detected by a hand-held device.

Lackowicz's group described boronic acid fluorophores (BAFs), which undergo spectral

changes in the presence of sugars, leading to a change in fluorescence intensity and wavelength upon binding to D-fructose.[170] The binding affinity decreases for D-galactose and D-glucose. These BAF probes showed wavelength shifts and intensity changes when embedded in a commercial contact lens (a polyvinyl alcohol-type photo-cured polymer) and immersed in glucose solutions. The probes included stilbene, polyene, and chalcone derivatives. Examples of BAF probes are 4′-dimethylaminostilbene-4-boronic acid, 4′-cyanostilbene-4-boronic acid, and 1-(*p*-boronophenyl)-4-(*p*-dimethylaminophenyl)buta-1,2-diene. Stilbene polyene derivatives were excited at 320–340 nm, while chalcone derivatives were excited at 430 nm.[170] Argose, Inc. explored the use of fluorescence for the NI determination of glucose in the skin.[171] Fluorescence methods that depend on interaction between glucose and a specific binding molecule, such as boronic acid and con-A, or are involved in a metabolic pathway will have a specificity advantage, when successfully applied *in vivo*.

Use of photonic crystals

Asher's group has developed a photonic sensing material that responds to analyte concentrations via diffraction of visible light from polymerized crystalline colloidal arrays (PCCAs).[172,173] PCCAs are periodic crystalline colloidal arrays (CCAs) of spherical polystyrene colloids polymerized within thin hydrogel films. The CCAs are brightly colored as they diffract visible light due to Bragg's diffraction.[172–177]

Bragg diffraction depends on the refractive index of the system (solvent, hydrogel, and colloids), the spacing d between the diffracting planes. The array will act as a diffraction grating for white light, allowing a specific diffracted wavelength λ to be detected at a specific glancing angle between the incident light propagation direction and the diffracting planes. Incorporation of charged species, or change in electric charge in the PCCAs, causes the arrays to expand, changing the spacing d. The diffraction pattern then changes causing a wavelength shift in the light reflected off the array.[172–177]

Several studies show the ability of the PCCA films to detect metal ions,[174] creatinine,[175] and glucose.[176,177] Asher's group constructed a glucose photonic sensor in the form of a thin acrylamide diffracting PCCA hydrogel film that contains glucose oxidase or phenyl boronic acid crystals as the molecular recognition elements. Attachment of glucose causes change in charge distribution. Glucose capture by glucose oxidase, or phenyl boronic acid, results in change in the spacing d in the Bragg equation, causing shifts in wavelengths of diffracted light. For example, 0.1 mmol/L glucose causes the diffracted light to shift from yellow at 550 nm to red at 600 nm. The diffraction spectral shift responds to change in glucose concentration in *in vitro* experiments. The plot shows a high sensitivity to glucose concentration between 0 and 10 mmol/L.[176,177]

The polymer film sensor is conceived to be used as a contact lens, which changes color according to the glucose concentration in tears. The use of glucose oxidase or phenyl boronic acid to capture glucose from tears has specificity advantages. The polymer film methods measure glucose in tears; the relative concentration and lag time between glucose concentration in blood and in tears require detailed studies.

NON-OPTICAL METHODS FOR THE NI DETERMINATION OF GLUCOSE

Impedance measurements

Measurement of tissue and cell impedance at different frequencies of an oscillating alternating current field yields the dielectric permeability of the cell membranes. The plot of the dielectric permeability $\varepsilon^*(\omega)$ at the different oscillation frequencies is the dielectric spectrum of the sample, where ω is the oscillation frequency in Hz (cycles per second). The dielectric spectrum is measured over a frequency range of 100 Hz to 100 MHz (10^2–10^8 oscillations per second).[178–183] The frequency distribution and the magnitude of $\varepsilon^*(\omega)$ were measured for a suspension of RBCs in glucose solutions. Both frequency distribution and magnitude of $\varepsilon^*(\omega)$ were dependent on the concentration of the metabolically active enan-

tiomer D-glucose, but were independent of the concentration of the metabolically inactive enantiomer L-glucose.[183]

Changes in blood glucose concentration induce changes in cells involved in carbohydrate metabolism. Hillier *et al*.[178] studied the effect of hyperglycemia in decreasing the Na^+ concentration in healthy subjects under insulin deficiency conditions. In addition to its role in inducing hyperglycemia, insulin deficiency reduces the permeability of most cells to glucose and accentuates its osmotic effect. Mean serum Na^+ and plasma glucose concentrations for six healthy fasting volunteers, who were given somatostatin to suppress insulin secretion, were determined in a glucose infusion experiment. Infused glucose brought up its blood concentration to 33.3 mmol/L within an hour, and then glucose infusion was stopped and insulin was infused to lower the blood glucose concentration to 7.78 mmol/L. As shown in Figure 7, serum glucose is reversibly related to Na^+ concentration. The decrease in Na^+ concentration as a result of increased glucose was less pronounced when glucose was infused without suppressing endogenous insulin secretion.[180]

RBCs undergo a decrease in sodium ion concentration and an increase in potassium ion concentrations due to water movement from RBCs to plasma, induced by change in glucose concentration.[178] Variation in electrolyte balance in blood causes change in RBC membrane potential, which can be followed by determining the permittivity and conductivity of cell membranes using time domain dielectric spectroscopy.[181,182]

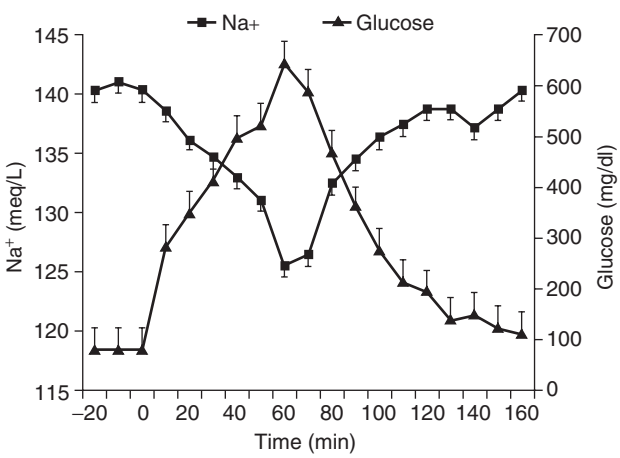

FIG. 7. Mean values serum sodium and plasma glucose concentrations for six healthy adults in a glucose infusion experiment. Subjects were fasting and were given somatostatin to suppress insulin secretion. Glucose concentration was increased to 33 mmol/L within an hour and then stopped. Reproduced with permission from Caduff *et al*.[179]

Suspensions of human RBCs in phosphate-buffered saline solution containing variable concentrations of D-glucose or L-glucose of constant osmolality showed a spike in $\varepsilon^*(\omega)$ at a D-glucose concentration of 12 mmol/L and no such effect when L-glucose was used. This shows an interesting specificity for the metabolically active enantiomer.[183]

Changes in the glucose concentrations were monitored in an NI experiment by varying the frequency in the radio band over a range that was optimized to measure the impact of glucose on the impedance pattern.[179] A number of human hyperglycemic excursion measurements were performed with healthy volunteers using a wristwatch-size sensor, which holds an open resonant circuit coupled to the skin and a circuit[179]:

1. The impedance sensor signals were correlated with changes in blood glucose or glucose in the ISF during a glucose clamp. A microdialysis catheter abdominally placed in the subcutaneous tissue measured blood glucose and glucose changes in ISF. Blood glucose was increased rapidly in eight healthy subjects from 5.56 to 16.67 mmol/L. A good correlation between changes in blood glucose and sensor recordings was reported in five out of the eight experiments. The profile for the glucose changes in the ISF is superimposed as well, showing the typical lag time between changes of glucose in blood and ISF.
2. An oral glucose load was administered to four healthy subjects to raise its values in blood from 5.56 to 16.67 mmol/L. The baseline was set by infusion of somatostatin to suppress endogenous insulin secretion. Three out of the four experiments showed a good correlation between changes in blood glucose and the sensor signals.
3. Sensor signals over time were recorded while blood glucose remained unchanged.

Blood glucose was kept constant for 8 h in four healthy subjects in order to study changes in the impedance pattern, which might occur over time. In 75% of the experiments glucose changes could be closely tracked. Only small changes occurred in the sensor signal over time.

The results of this human experiment showed a proof of concept for this non-optical, NI monitoring approach.[179] It is attractive as a continuous glucose monitoring method. Because of the indirect nature of this measurement, a number of questions remain to be clarified, such as the effect of body water content or dehydration on this measurement. There is a dehydrating effect that accompanies hyperglycemia.[178] Some of the co-morbidities that affect cell membranes were listed in the section discussing RBC light scattering.

Tissue temperature measurements

Cho and Holzgreve[184,185] proposed a different non-optical technique that is based on body thermal effects. Measurement of body temperature was suggested as an NI method to determine glucose in the blood. The method is based on measuring body temperature at an extremity, such as the forefinger, using contact and non-contact temperature measuring techniques and correlating a mathematical function of the measured temperature with glucose concentration. Body temperatures at extremities depend on environmental temperature, activity, time from meal, alcohol and nicotine consumption, and other disease states.[184,185] Accurate measurement of changes in body temperature was claimed to yield NI glucose calibration plots.[184,185] It is difficult to separate circadian temperature periodicity from temperature change because of the glucose concentration effect. Thermal variations that characterize tissue metabolism have circadian periodicity and are not related to glucose metabolism only, but can be associated with other physiological effects or disease states. Circadian variations in body temperature have been discussed.[27,28] Temperature changes upon glucose ingestion.[29] The tympanic membrane is a better measurement site because of the absence of the SC, calluses, and variable skin thickness, which can affect temperature measurements.

A new publication has described a method for combining temperature measurements with optical measurements for NI determination of glucose.[186] The method is suggested to depend on measurement of blood flow, as gauged by temperature, and blood oxygenation is determined from the optical measurements. The various physical parameters are used to calculate glucose concentration, presumably based on the generated metabolic heat. The experimental details and calibration methods and algorithm used are not described in this short communication.[186]

The relationship between glucose concentration and blood flow was not established. There are specific issues associated with blood flow in patients with diabetes. LDF studies showed an impaired decrease in cutaneous blood flow and difference in blood flow response to cooling or warming in patients with diabetes.[47–49] Patients with diabetes exhibited differences from subjects without diabetes in cutaneous blood flow,[52–55] and in response to contralateral cooling.[58] Both insulin and glucose are reported to have vascular activities affecting blood flow.[62–64] The relationship between oxygen saturation and glucose concentration is not established in any of the previous studies. In the absence of corroborating studies, it is possible to interpret the published Clarke error grid as representing an overmodeled calibration relationship.

Table 7 summarizes the reported TGS,[153] thermal emission,[154] impedance frequency,[179] temperature measurement,[185] and the method proposed by Ko *et al.*[186] that combines temperature, blood flow and oxygen saturation measurement, and non-optical methods.

CONCLUSIONS AND AUTHOR'S VIEWS

In addition to the emergence of new detection methods, improvements in the measurement technologies and methods to reduce noise in NI glucose measurement were pursued. Advances were made in understanding and resolving the specificity, compartmentalization, and calibration issues of NI glucose measurements.

Table 7. Mid-IR Thermal Emission and Nonoptical Methods

Method	*Reference*	*Specificity*	*Compartmentalization*	*Calibration*
Thermal gradient spectroscopy (TGS)	Klonoff *et al.*[153]; Zheng *et al.*[154]	Mid-IR glucose-specific emission band	ISF fluid in cutaneous layer, forearm	Calibration model
Thermal emission	Malchoff *et al.*[158]	Glucose-specific emission band	Tympanic membrane	Calibration model, prediction
Impedance frequency	Hillier *et al.*[178]; Caduff *et al.*[179]	Effect of D-glucose on cell membrane	Vascular system, wrist	Calibration model
Temperature	Cho and Holzgreve[184,185]	Effect of glucose on body temperature	Finger	Calibration model
Temperature, blood flow, and oxygen saturation	Ko *et al.*[186]	Effect of glucose on temperature, blood flow, and oxygen saturation	Finger	Calibration model

Specificity of NI glucose measurements

The issue of specificity of measuring a glucose molecular property is still unresolved, at least in a commercial product. Most NI techniques provide indirect evidence that the measured signal is related to a molecular property of glucose. Multivariate techniques are used to extract glucose concentration and to establish correlation between signal and glucose values to compensate for lack of specificity; this is especially true of NIR measurements, but to a lesser extent for mid-IR spectroscopy. The availability of a large number of reported NIR studies, and limited number of mid-IR studies, makes this conclusion rather tenuous. The interplay among *in vitro* experiments, *in vivo* experiments, and simulation studies is used to prove the specificity of some methods. OGTT and MTT results can have coincidental overlap with physiologic events. A way to improve glucose correlation is to experimentally suppress coincidental correlations and minimize measurement noise.

There are significant advances in methods that depend on measuring the effect of glucose on properties of tissue or blood. The PA effect took a different turn from measuring light absorption to tracking scattering effects. Fluorescence measurements appeared on the horizon. Fluorescence and photonic crystal diffraction methods that depend on interaction between glucose and a specific binding molecule or a metabolic pathway will have a specificity advantage, when successfully applied *in vivo*.

Compartmentalization of glucose values

The precision and specificity of the NI measurements do not yet allow determination of differences in glucose concentrations in body compartments. Several techniques target specific body compartments. Transmission and diffuse reflectance measurements track glucose concentrations in the vascular bed, while localized reflectance and frequency domain methods detect change in glucose concentration in the ISF via its effect on μ_s'. New methods target the vascular compartment, the dermis, tympanic membrane, and AH. Methods that depend on using a contact lens-type membrane will be dealing with the tears as a body fluid in the extracorporeal compartment.

Calibration of NI glucose devices

It is possible to track changes in glucose concentration during a glycemic swing using current methods. Chemometric methods are necessary for data analysis in some technologies, and it is important to guard against overfitting. Calibration should allow a random spot testing as well as sequential continuous monitoring of glucose, and be easily but not frequently updated. It should cover multiple physiological disease, environmental, and activity condi-

tions. Researchers should strive to achieve multipatient calibration, which requires understanding the physical and physiological factors affecting the signals, interperson differences, and measurement of noise. It is preferable to have a self-calibrating detection method that yields a universal calibration model, which is not unique to an individual and does not require multiple invasive data points and chemometric methods. Available clinical data do not show this with great certainty for any method.

Most of the reported methods relied on hyperglycemic excursion and multivariate calibration, thus raising two issues. The first one is the accuracy of glucose invasive measurements and implanted sensors are problematic in the hypoglycemic range. This observation led Klonoff[187] to suggest a different metric for the hypoglycemic range. A second issue is that multivariate analysis leads to one standard error value across the whole glucose concentration range. This SEP will be smaller than the commonly used standard deviation at high glucose concentration. But it will be larger than it is at low glucose concentration, leading to higher error in the hypoglycemic range.

ACKNOWLEDGMENTS

Thanks to my colleagues at Abbott Laboratories—Shu-jen Yeh, Charles Hanna, Michael Lowery, Ronald Hohs, Brenda Calfin, Xiaomao Wu, Tzyy-Wen Jeng, Stan Kantor, James Babb, Gary Oosta, and Eric Shain—who helped me navigate through the minefield of NI glucose testing.

REFERENCES

1. Khalil OS: Spectroscopic and clinical aspects of noninvasive glucose measurements. Clin Chem 1999; 45:165–177.
2. McNichols RJ, Cote GL: Optical glucose sensing in biological fluids. J Biomed Opt 2000;5:5–16.
3. Koschinsky T, Heinemann L: Sensors for glucose monitoring: technical and clinical aspects. Diabetes Metab Res Rev 2001;17:113–123.
4. Gutman S, Bernhardt P, Pinkos A, Moxey-Mims M, Knott T, Cooper J: Regulatory aspects of noninvasive glucose measurements. Diabetes Technol Ther 2002;4:779–781.
5. Heinemann L, Koschinsky T: Continuous glucose monitoring: an overview of today's technologies and their clinical applications. Int J Clin Pract Suppl 2002;129:75–79.
6. Koschinsky T, Jungheim K, Heinemann L: Glucose sensors and alternate site testing-like phenomenon: relationship between rapid blood glucose changes and glucose sensor signals. Diabetes Technol Ther 2003;5:829–842.
7. Thennadil SN, Rennert JL, Wenzel BJ, Hazen KH, Ruchti TL, Block MB: Comparison of glucose concentration in interstitial fluid, and capillary and venous blood during rapid changes in blood glucose levels. Diabetes Technol Ther 2001;3:357–365.
8. Boyne MS, Silver DM, Kaplan J, Saudek D: Timing of changes in interstitial and venous blood glucose measured with a continuous subcutaneous glucose sensor. Diabetes 2003;52:2790–2794.
9. Rebrin K, Steil GM, van Antwerp WP, Mastrototaro JJ: Subcutaneous glucose predicts plasma glucose independent of insulin: implications for continuous monitoring. Am J Physiol 1999;277:E561–E571.
10. Maruo K, Tsurugi M, Tamura M, Ozaki Y: In vivo noninvasive measurement of blood glucose by near-infrared diffuse-reflectance spectroscopy. Appl Spectrosc 2003;57:1236–1244.
11. Yeh S-j, Hanna CF, Khalil OS: Monitoring blood glucose changes in cutaneous tissue by temperature-modulated localized reflectance measurements. Clin Chem 2003;49:924–934.
12. Malin SF, Ruchti TL, Blank TB, Thennadil SN, Monfre SL: Noninvasive prediction of glucose by near-infrared diffuse reflectance spectroscopy. Clin Chem 1999;45:1651–1658.
13. Rosenthal RD, Paynter LN, Mackie LH, inventors; Futrex, Inc., assignee: Non-invasive measurements of blood glucose. US patent 5,028,787. July 2, 1991.
14. Rosenthal RD, Paynter LN, Mackie LH, inventors; Futrex, Inc., assignee: Non-invasive measurements of blood glucose. US patent 5,086,229. February 4, 1992.
15. Gabriely I, Wozniak R, Mevorach M, Kaplan J, Aharon Y, Shamoon H: Transcutaneous glucose measurement using near infrared spectroscopy during hypoglycemia. Diabetes Care 1999;22:2026–2032.
16. Finarov A, Kleinman Y, Fine I, inventors; Orsense Ltd., assignee: Optical device for non-invasive measurement of blood related signals utilizing a finger holder. US patent 6,213,952. April 10, 2001.
17. Harjunmaa H, Peura PA, Mendelson Y, inventors; Worcester Polytechnic Institute, assignee: Method and apparatus for measuring the concentration of absorbing substances. US patent 5,112,124. May 12, 1992.
18. Peters RK, Elmerick D, inventors; Emerging Technology Systems, assignee: Non-invasive glucose measuring device and method for measuring blood glucose. US patent 5,910,109. June 8, 1999.
19. Burmeister JJ, Arnold MA, Small GW: Noninvasive blood glucose measurements by near-infrared trans-

mission spectroscopy across human tongues. Diabetes Technol Ther 2000;2:5–16.
20. Heinemann L, Schmelzeisen-Redeker G: Non-invasive continuous glucose monitoring in Type I diabetic patients with optical glucose sensors. Non-Invasive Task Force (NITF). Diabetologia 1998;41:848–854.
21. Heise HM, Marbach R: Human oral mucosa studies with varying blood glucose concentration by non-invasive ATR-FT-IR-spectroscopy. Cell Mol Biol (Noisy-le-grand) 1998;44:899–912.
22. Rabinovitch B, March WF, Adams RL: Noninvasive glucose monitoring of the aqueous humor of the eye: I. Measurement of very small optical rotations. Diabetes Care 1982;5:254–258.
23. Abreu MM, inventor: Contact device for application in direct apposition to the conjunctive of the eye. US patent 6,312,393. November 6, 2001.
24. Martens H, Naes T: Multivariate Calibration. New York: John Wiley and Sons, 1989.
25. Haaland DM, Easterling RG: Application of new least squares analysis methods for the quantitative analysis of multicomponent samples. Appl Spectrosc 1982;36:665–673.
26. Haaland DM, Easterling RG, Vopicka DA: Multivariate least-squares methods applied to quantitative spectral analysis of multicomponent samples. Appl Spectrosc 1985;39:73–84.
27. Seaman GV, Engel R, Swank RL, Hissen W: Circadian periodicity in some physicochemical parameters of circulating blood. Nature 1965;207:833–835.
28. Deryagina GP, Kraevskii YM: Circadian rhythm of body temperature, blood pressure, and heart rate. Hum Physiol 1983;9:133–140.
29. Hillson RM, Hockaday TD: Facial and sublingual temperature changes following intravenous glucose injection in diabetics. Diabet Metab 1982;8:15–19.
30. Clemens AH, Chang PH, Myers RW: The development of Biostator, a glucose controlled insulin infusion system (GCIIS). Horm Metab Res Suppl 1977; 7:23–33.
31. DeFronzo RA, Tobin JD, Andres R: Glucose clamp technique: a method for quantifying insulin secretion and resistance. Am J Physiol 1979;237:E214–E223.
32. Clemens AH, Hough DL, D'Orazio PA: Development of the Biostator glucose clamping algorithm. Clin Chem 1982;28:1899–1904.
33. Arnold MA, Burmeister JJ, Small GW: Phantom glucose calibration models from simulated noninvasive human near infrared spectra. Anal Chem 1998;70: 1773–1781.
34. Samann A, Fischbacher CH, Jagemann KU, Danzer K, Schuler J, Papenkordt L, Muller UA: Non-invasive blood glucose monitoring by means of near infrared spectroscopy: investigation of long-term accuracy and stability. Exp Clin Endocrinol Diabetes 2000;108:406–413.
35. Wilson B: Measurement of tissue optical properties: methods and theories. In: Welch AJ, Van Gemert MCC, eds.: Optical-Thermal Response of Laser-Irradiated Tissue. New York: Plenum Press, 1995:233–261.
36. Murrer LH, Marijnissen HP, Star WM: Monte Carlo simulations for EndoBronchial Photodynamic Therapy: the influence of variations in optical and geometrical properties and of realistic and eccentric light sources. Lasers Surg Med 1998;22:193–206.
37. de Mul FF, Steenbergen W, Greve J: Doppler Monte Carlo simulations of light scattering in tissue to support laser-Doppler perfusion measurements. Technol Health Care 1999;7:171–183.
38. Pavlin M, Jarm T, Miklavcic D: Monte-Carlo simulation of light transport for NIRS measurements in tumors of elliptic geometry. Adv Exp Med Biol 2003; 530:41–49.
39. Youcef-Toumi Y, Saptari VA: Noninvasive blood glucose analysis using near infrared absorption spectroscopy. Progress Report MIT Home Automation and Healthcare Consortium 1999. Available online at: http//darbeloffllab.mit.edu.home automation/ report2-4/.
40. Graaff R, Aarnoudse JG, Zijp JR, Sloot PMA, de Mul FFM, Greve J, Koelink MH: Reduced light-scattering properties for mixture of spherical particles: a simple approximation derived from Mie calculations. Appl Opt 1992;31:1370–1376.
41. Vasko PD, Blackwell J, Koenig JL: Infrared and Raman spectroscopy of carbohydrates. I: Identification of O-H and C-H vibrational modes for D-glucose, malose, cellobiose, and dextran by deuterium substitution methods. Carbohydr Res 1971;19:297–310.
42. Vasko PD, Blackwell J, Koenig JL: Infrared and Raman spectroscopy of carbohydrates. II: Normal coordinate analysis of α-D-glucose. Carbohydr Res 1972;23:407–417.
43. Lucassen GW, Caspers PJ, Puppels GJ: Infrared and Raman spectroscopy of human skin in vivo. In: Tuchin VV, ed. Handbook of Optical Biomedical Diagnostics. Bellingham, WA: SPIE Press, 2002:787–823.
44. Lucassen GW, van Veen GNA, Jansen JAJ: Band analysis of hydrated human skin stratum corneum attenuated total reflectance Fourier transform infrared spectra in vivo. J Biomed Opt 1998;3:267–280.
45. Brancaleon L, Bamberg MP, Sakamaki T, Kollias N: Attenuated total reflection-Fourier transform infrared spectroscopy as a possible method to investigate biophysical parameters of stratum corneum in vivo. J Invest Dermatol 2001;116:380–386.
46. Brancaleon L, Bamberg MP, Sakamaki T, Kollias N: Spectral differences between stratum corneum and sebaceous molecular components in the mid-IR. Appl Spectrosc 2000;54:1175–1182.
47. Rendell M, Bergman T, O'Donnell G, Drobny E, Borgos J, Bonnor R: Microvascular blood flow, volume, and velocity, measured by laser Doppler techniques in IDDM. Diabetes 1989;38:819–824.
48. Rendell M, Bamisedun O: Diabetic cutaneous microangiopathy. Am J Med 1992;93:611–618.

49. Wilson SB: Detection of microvascular impairment in type-1 diabetes by laser Doppler flowmetry. Clin Physiol 1992;12:195–208.
50. Braverman IM, Keh-Yen A: Ultrastructural abnormalities of the microvasculature and elastic fibers in the skin of juvenile diabetics. J Invest Dermatol 1984;82:270–274.
51. Rayman G, Williams SA, Spenser PD, Smajie LH, Wise PH, Tooke JE: Impaired microvascular hyperemic response to minor skin trauma in type-1 diabetes. Br Med J (Clin Res Ed) 1986;292:1295–1298.
52. Khan F, Elhadd T, Green SA, Belch J: Impaired skin microvascular function in children, adolescent, and young adults with type-1 diabetes. Diabetes Care 2000;23:215–220.
53. Tooke JE, Ostergren J, Lins P-E, Fragrell B: Skin microvascular blood flow control in long duration diabetics with and without complications. Diabetes Res 1987;5:189–192.
54. Salomaa V, Riley W, Kark JD, Nardo C, Folsom AR: Non-insulin-dependent diabetes mellitus and fasting glucose and insulin concentrations are associated with arterial stiffness indexes. The ARIC Study. Atherosclerosis Risk in Communities Study. Circulation 1995;91:1432–1443.
55. Hassan AAK, Tooke J: Effect of change in local skin temperature on postural vasoconstriction in man. Clin Sci 1988;74:201–206.
56. Jaap AJ, Hammersley MS, Shore AC, Tooke JE: Reduced microvascular hyperemia in subjects at risk of developing Type-2 (non-insulin-dependent) diabetes mellitus. Diabetologia 1994;37:214–216.
57. Stansberry KB, Shapiro SA, Hill MA, McNitt PM, Meyer MD, Vinik AI: Impaired peripheral vasomotion in diabetes. Diabetes Care 1006;19:715–721.
58. Haak E, Haak T, Grozinger Y, Krebs G, Usadel KH, Kusterer K: The impact of contralateral cooling of skin capillary blood cell velocity in patients with diabetes mellitus. J Vasc Res 1998;35:245–249.
59. Akbari CM, Saouaf R, Barnhill DF, Newman PA, LoGerfo FW, Veves A: Endothelium-dependent vasodilatation is impaired in both microcirculation and macrocirculation during acute hyperglycemia. J Vasc Surg 1998;28:687–694.
60. Caballero AE, Arora S, Saouaf R, Lim SC, Smakowski P, Park JY, King GL, LoGerfo FW, Horton ES, Veves A: Microvascular and macrovascular reactivity is reduced in subjects at risk for type-2 diabetes. Diabetes 1999;48:1856–1862.
61. Wiernsperger N: Defects in microvascular heamodynamics during prediabetes: Contributor or epiphenomenon? Diabetologia 2000;43:1439–1449.
62. Williams SB, Goldfine AB, Timimi FK. Ting HH, Roddy M-A, Simonson DC, Creager MA: Acute hyperglycemia attenuates endothelium-dependent vasodilation in humans in vivo. Circulation 1998;97: 1695–1701.
63. Yki-Jarvinen H, Utriainen T: Insulin-induced vasodilatation: physiology or pharmacology. Diabetologia 1998;41:369–379.
64. Oomen PHN, Kant GD, Dullaart RPF, Reitsma WD, Smit AJ: Acute hyperglycemia and hyperinsulinemia enhance vasodilatation in Type-1 diabetes mellitus without increasing capillary permeability and inducing endothelial dysfunction. Microvasc Res 2002; 63:1–9.
65. MacGregor AR, inventor: Method and apparatus for non-invasively determining blood analytes. US patent 5,617,852. April 8, 1997.
66. Rendell M, Hovelson C, O'Connor K, Cheung L, Huard S, Kong TS, Catania A, Rosenthal R: Determination of blood flow in the finger using near-infrared spectroscopy. Clin Physiol 1998;18:426–434.
67. Wu X, Yeh S-j, Jeng T-W, Khalil OS: Noninvasive determination of hemoglobin and hematocrit using a temperature-controlled localized reflectance tissue photometer. Anal Biochem 2000;287:284–293.
68. Rendell M, Anderson E, Schlueter W, Mailliard J, Honigs D, Rosenthal R: Determination of hemoglobin levels in the finger using near infrared spectroscopy. Clin Lab Haematol 2003;25:93–97.
69. Sibbald RG, Landolt SJ, Toth D: Skin and diabetes. Endocrinol Metab Clin North Am 1996;25:463–472.
70. Monnier VM, Bautista O, Kenny D, Sell DR, Fogarty J, Dahms W, Cleary PA, Lachin J, Genuth S: Skin collagen glycation, glycoxidation, and crosslinking are lower in subjects with long-term intensive versus conventional therapy of type-1 diabetes: relevance of glycated collagen products versus HbA1c as markers for diabetic complications. Diabetes 1999;48:870–880.
71. James VJ, Belbridge L, McLennan SV, Yue DK: Use of X-ray diffraction in study of human diabetic and aging collagen. Diabetes 1999;40:391–394.
72. Firsov NN, Priezzhev AV, Ryaboshapka OM, Sirko IV: Aggregation and disaggregation of erythrocytes in whole blood: study by back scattering technique. J Biomed Opt 1999;4:76–84.
73. Priezzhev AV, Firsov NN, Landman J: Light backscattering diagnostics of red blood cell aggregation in whole blood samples. In: Tuchin VV, ed. Handbook of Optical Biomedical Diagnostics. Bellingham, WA: SPIE Press, 2002:651–674.
74. Landman J, Weigmann, H-J, Sterry W, Keisewetter H, RogganA, Muller G, Priezzhev AV, Firsov AN: Investigation of the aggregation and disaggregation properties of erythrocytes by light scattering measurements. Proc SPIE 2000;3923:26–31.
75. Shvartsman LD, Fine I: RBC aggregation effects on light scattering from blood. Proc SPIE 2000;2162: 120–129.
76. Mazarevica G, Freivalds T, Jurka A: Properties of erythrocyte light refraction in diabetic patients. J Biomed Opt 2002;7:244–247.
77. Fusman R, Rotstein R, Elishkewich K, Zeltser D, Cohen S, Kofler M, Avitzour D, Arber N, Berliner S, Shapirea I: Image analysis for the detection of increased erythrocyte, leukocyte and platelet adhesiveness/aggregation in the peripheral blood of patients with diabetes mellitus. Acta Diabetol 2001;38: 129–134.

78. Cicha I, Suzuki Y, Tateishi N, Maeda N: Enhancement of red blood cell aggregation by plasma triglycerides. Clin Hemorheol Microcirc 2001;24:247–255.
79. Ercan M, Konukoglu D, Erdem T, Onen S: The effects of cholesterol levels on hemorheological parameters in diabetic patients. Clin Hemorheol Microcirc 2002;26:257–263.
80. Yedgar S, Koshkaryev A, Barshtein G: The red blood cell in vascular occlusion. Pathophysiol Haemost Thromb 2002;32:263–268.
81. Ami RB, Barshstein G, Zeltzer D, Goldberg Y, Shapira I, Roth A, Keren G, Miller H, Prochorov V, Eldor A, Berliner S, Yedgar S: Parameters of red blood cell aggregation as correlates of the inflammatory state. Am J Physiol Heart Circ Physiol 2001;280:H1982–H1988.
82. Firsov NN, Bjelle A, Korotaeva TV, Priezzhev AV, Ryaboshapka OM: Clinical applications of the measurements of spontaneous erythrocyte aggregation and disaggregation. A pilot study. Clin Hemorheol Microcirc 1998;18:87–97.
83. Yeh S-j, Khalil OS, Hanna CF, Kantor S, Wu X, Jeng T-W, Bolt RA: Temperature dependence of optical properties of in-vivo human skin. Proc SPIE 2001; 4250:455–461.
84. Khalil OS, Yeh S-j, Lowery MG, Wu X, Hanna CF, Kantor S, Jeng T-W, Kanger J, Bolt RA, de Mul FF: Temperature modulation of optical properties of human skin. J Biomed Opt 2003;8:191–205.
85. Yeh S-j, Khalil OS, Hanna CF, Kantor S: Near infrared thermo-optical response of the localized reflectance of intact diabetic and non-diabetic human skin. J Biomed Opt 2003;8:534–544.
86. Khalil OS, Yeh S-j, Wu X: Response of near IR localized reflectance signals of intact diabetic human skin to thermal stimuli. Proc SPIE 2003;5086:142–148.
87. Yeh S-j, Hanna CF, Kantor S, Hohs R, Khalil OS: Differences in thermal optical response between intact diabetic and no diabetic human skin. Proc SPIE 2003;4958:213–224.
88. Elsner P, Berardesca E, Maibach HI, eds.: Bioengineering of the Skin: Water and the Stratum Corneum, Vol. 1. Boca Raton, FL: CRC Press, 1994.
89. Blank TB, Ruchti TL, Lorenz AD, Monfre SL, Makarewicz MR, Mattu M, Hazen KH: Clinical results from non-invasive blood glucose monitor. Proc SPIE 2002;4624:1–10.
90. Burmeister JJ, Arnold MA: Evaluation of measurement sites for noninvasive blood glucose sensing with near-infrared transmission spectroscopy. Clin Chem 1999;45:1621–1627.
91. Heise HM, Bittner A, Marbach R: Clinical chemistry and near infrared spectroscopy: technology for noninvasive glucose monitoring. J Infrared Spectrosc 1998;6:349–359.
92. Heise HM, Bittner A, Marbach R: Near-infrared reflectance spectroscopy for noninvasive monitoring of metabolites. Clin Chem Lab Med 2000;38:137–145.
93. Heise HM, Lampen P: Transcutaneous glucose measurements using near-infrared spectroscopy: validation of the statistical calibration models. Diabetes Care 2000;23:1208–1209.
94. Gabriely I, Shamoon H: Transcutaneous glucose measurement using near-infrared spectroscopy during hypoglycemia. Diabetes Care 2000;23:1209–1210.
95. Maruo K, Chin J, Tamura M: Non-invasive blood glucose monitoring by novel fiber optical probe. Proc SPIE 2001;4264:20–27.
96. Janatsch G, Kruse-Jarres JD, Marbach R, Heise HM: Multivariate calibration for assays in clinical chemistry using attenuated total reflection infrared spectra of human blood plasma. Anal Chem 1989;61: 2016–2023.
97. Deissel F, Willman S, Kamphaus P, Kurte R, Damm U, Heise HM: Glucose quantification in dried-down samples using mid-infrared attenuated total reflection spectroscopy. Appl Spectrosc 2004;58:422–450.
98. Petrich W, Dolenk B, Früh J, Ganz M, Greger H, Jacob S, Keller F, Nikulin AE, Otto, M, Quarder O, Somorjai R.L, Staib A, Warner G, Wielinger H: Disease pattern recognition in infrared spectra of human sera with diabetes mellitus as an example. Appl Opt 2000; 39:3372–3379.
99. Kim YJ, Hahn S, Yoon G: Determination of glucose in whole blood samples by mid-infrared spectroscopy. Appl Opt 2003;42:745–749.
100. Shen YC, Davies AG, Linfield EH, Elsey TS, Taday PF, Arnone AD: The use of Fourier-transform infrared spectroscopy for the quantitative determination of glucose concentration in whole blood. Phys Med Biol 2003;48:2023–2032.
101. Haaland DM, Robinson MR, Koepp GW, Thomas EV, Robinson PL, Eaton RP: Reagentless near infrared determination of glucose in whole blood using multivariate calibration. Appl Spectrosc1992;46: 1575–1578.
102. Ward KJ, Haaland DM, Robinson MR, Eaton RP: Post-prandial blood glucose determination by quantitative mid-infrared spectroscopy. Appl Spectrosc 1992;46:959–965.
103. Berman HL, Roe JN, inventors; MedOptix, Inc., assignee: Cleaning system for infrared ATR glucose measurement system (II). US patent 6,362,144. March 26, 2002.
104. Berman HL, Roe JN, inventors; MedOptix, Inc., assignee: Infrared ATR glucose measurement system having an ATR with mirrored ends. US patent 6,421,548. July 16, 2002.
105. Berman HL, Roe JN, inventors; MedOptix, Inc., assignee: Method for preparing skin surface and determining glucose levels from that system. US patent 6,424,848. July 23, 2002.
106. Bruulsema JT, Hayward JE, Farrell T, Patterson M, Heinemann L, Berber M: Correlation between blood glucose concentration in diabetics and noninvasively measured tissue optical scattering coefficient. Opt Lett 1997;22:190–192.
107. Heinemann L, Kramer U, Klotzer HM, Hein M, Volz D, Hermann M, Heise T, Rave K: Non-Invasive Task Force: noninvasive glucose measurement by moni-

toring of scattering coefficient during oral glucose tolerance tests. Diabetes Technol Ther 2000;2:211–220.
108. Maier J, Walker S, Fantini S, Franceschini M, Gratton E: Non-invasive glucose determination by measuring variations of the reduced scattering coefficient of tissues in the near-infrared. Opt Lett 1994;19:2062–2064.
109. Bulow J, Astrup A, Christensen NJ, Kastrup J: Blood flow in skin, subcutaneous adipose tissue and skeletal muscle in the forearm of normal man during an oral glucose load. Acta Physiol Scand 1987;130:657–661.
110. Shvartsman LD, Fine I: Light scattering changes caused by RBC aggregation; physical basis for new approach to non-invasive blood count. Proc SPIE 2001;4263:131–142.
111. Cohen O, Fine I, Monashkin E, Karasik A: Glucose correlation with light scattering patterns—a novel method for non-invasive glucose measurements. Diabetes Technol Ther 2003;5:11–17.
112. Shvartsman LD, Fine I: Optical transmission of blood: effect of erythrocyte aggregation. IEEE Trans Biomed Eng 2003;50:1026–1033.
113. Elishkevitz K, Fusman R, Koffler M, Shapirea I, Zeltser D, Avitzour D, Arber N, Berliner S, Rotstein R: Rheological determinations of red blood cell aggregation in diabetic patients in relation to their metabolic control. Diabet Med 2002;19:152–156.
114. Haung D, Swanson EA, Lin CP, Schuman JS, Stinson WG, Chang W, Hee MR, Flotte T, Gregory K, Puliafito CA, Fujimoto JG: Optical coherence tomography. Science 1991;254:1178–1181.
115. Schmitt JM: Optical coherence tomography (OCT): a review. IEEE J Selected Top Quantum Electron 1999; 5:1205–1215.
116. Knuttel A, Bohlau-Gadau M, Rist M, Welker P, Gogolin U, Kugler C: In vivo evaluation of layered scattering coefficients and refractive indices with OCT. Proc SPIE 1999;3597:324–334.
117. Knuttel A, Boehlau-Godau M: Spatially confined and temporally resolved refractive index scattering evaluation of human skin performed with optical coherence tomography. J Biomed Opt 2000; 5:83–92.
118. Essenpreis M, Knuttel A, Boecker D, inventors; Boehringer Mannheim GmbH, assignee: Method and apparatus for determining glucose concentration in a biological sample. US patent 5,710,630. January 20, 1998.
119. Larin KV, Eledrisi MS, Motamedi M, Esenaliev RO: Noninvasive blood glucose monitoring with optical coherence tomography: a pilot study in human subjects. Diabetes Care 2002;25:2263–2267.
120. Esenaliev RO, Larin KV, Larina IV, Motamedi M: Noninvasive monitoring of glucose concentration with optical coherence tomography. Opt Lett 2001; 26:992–994.
121. Larin K, Larina I, Motamedi M, Gelikonov Y, Kuranov R, Esenaliev RO: Potential application of optical coherence tomography for non-invasive monitoring of glucose concentrations. Proc SPIE 2001;4263: 83–90.
122. Larin KV, Motamedi M, Ashitkov TV, Esenaliev RO: Specificity of noninvasive blood glucose sensing using optical coherence tomography technique: a pilot study. Phys Med Biol 2003;48:1371–1390.
123. Rabinovitch B, March WF, Adams RL: Noninvasive glucose monitoring of the aqueous humor of the eye: Part I. Measurement of very small optical rotations. Diabetes Care 1982;5:254–258.
124. Rawer R, Stork W, Muller-Glaser KD: Polarimetric methods for measurement of intra ocular glucose concentration. Biomed Tech (Berl) 2002;47(Suppl 1 Pt 1):186–188.
125. Cameron BD, Gorde HW, Satheesan B, Cote GL: The use of polarized laser light through the eye for noninvasive glucose monitoring. Diabetes Technol Ther 1999;1:135–143.
126. Cameron BD, Baba JS, Cote GL: Measurement of the glucose transport time delay between the blood and aqueous humor of the eye for the eventual development of a noninvasive glucose sensor. Diabetes Technol Ther 2001;3:201–207.
127. Chou C, Lin PK: Noninvasive glucose monitoring with optical heterodyne technique. Diabetes Technol Ther 2000;2:45–47.
128. Lane JT, Toris CB, Nakhle SN, Chacko DM, Wang YL, Yablonski ME: Acute effects of insulin on aqueous humor flow in patients with type-1 diabetes. Am J Ophthalmol 2001;132:321–327.
129. Bockle S, Rovati L, Ansari RR: Polarimetric glucose sensing using Brewster-reflection off the eye lens: theoretical analysis. Proc SPIE 2002;4624:160–164.
130. Hanlon EB, Manoharan R, Koo TW, Shafer KE, Motz JT, Fitzmaurice M, Kramer JR, Itzkan I, Dasari RR, Feld MS: Prospects for in vivo Raman spectroscopy. Phys Med Biol 2000;45:R1–R59.
131. Steffes PG: Laser-based measurement of glucose in the ocular aqueous humor: an efficacious portal for determination of serum glucose levels. Diabetes Technol Ther 1999;1:129–133.
132. Berger AJ, Itzkan I, Feld MS: Feasibility of measuring blood glucose concentration by near-infrared Raman spectroscopy. Spectrochim Acta A Mol Biomol Spectrosc 1997;53A:287–292.
133. Berger AJ, Koo TW, Itzkan I, Feld MS: An enhanced algorithm for linear multivariate calibration. Anal Chem 1998:70;623–627.
134. Koo TW, Berger AJ, Itzkan I, Horowitz G, Feld MS: Reagentless blood analysis by near-infrared Raman spectroscopy. Diabetes Technol Ther 1999;1:153–157.
135. Borchert MS, Storrie-Lombardi MC, Lambert JL: A noninvasive glucose monitor: preliminary results in rabbits. Diabetes Technol Ther 1999;1:145–151.
136. Caspers PJ, Lucassen GW, Puppels GJ: Combined in vivo confocal Raman spectroscopy and confocal microscopy of human skin. Biophys J 2003;85:572–580.
137. Chaiken J., Finney WF, Peterson CM, Peterson KP, Knusdon PE, Weinstock RS, Lein P: Noninvasive, in vivo, tissue modulated near infrared vibrational

spectroscopic study of mobile and static tissues: blood chemistry. Proc SPIE 2000;3918:135–143.
138. Chaiken J, Finney WF, Knudson PE, Peterson KP, Peterson CM, Yang X, Weinstock RS: Progress in noninvasive, in-vivo, tissue modulated Raman spectroscopy of human blood. Proc SPIE 2001;4254: 216–227.
139. Haynes CL, Van Duyne RP: Plasmon-sampled surface-enhanced Raman excitation spectroscopy. J Phys Chem B 2003;107:7426–7433.
140. Schatz GC, Van Duyne RP: Electromagnetic mechanism of surface-enhanced spectroscopy. In: Chalmers JM, Griffiths PR, eds. Handbook of Vibrational Spectroscopy, Vol. 1. Wiley: New York, 2002: 759–774.
141. Shafer-Peltier KE, Haynes CL, Glucksberg MR, Van Duyne RP: Toward a glucose biosensor based on surface-enhanced Raman scattering. J Am Chem Soc 2003;125:588–593.
142. Yonzon CR, Haynes CL, Zhang X, Walsh JT, Van Duyne RP: A glucose biosensor based on surface-enhanced Raman scattering: improved partition layer, temporal stability, reversibility, and resistance to serum protein interference. Anal Chem 2004;76:78–85.
143. Tam AC, Patel CKN: Optical absorption of light and heavy water by laser photoacoustic spectroscopy. Appl Opt 1979;18:3348–3357.
144. MacKenzie HA, Ashton HS, Spiers S, Shen Y, Freeborn SS, Hannigan J, Lindberg J, Rae P: Advances in photoacoustic noninvasive glucose testing. Clin Chem 1999;45:1587–1595.
145. Fainchtein R, Stoyanov BJ, Murphy JC, Wilson DA, Hanley DF: Local determination of hemoglobin concentration and degree of oxygenation in tissue by pulsed photoacoustic spectroscopy. Proc SPIE 2000; 3916:19–33.
146. Bednov AA, Karabutov AK, Savateeva EV, March WF, Oraevsky AA: Monitoring glucose in vivo by measuring laser-induced acoustic profiles. Proc SPIE 2000;3916:9–18.
147. Zhao Z, Myllylä R: Photoacoustic determination of glucose concentration in whole blood by a near-infrared laser diode. Proc SPIE 2001;4256:77–83.
148. Zhao Z: Pulsed photoacoustic techniques and glucose determination in human blood and tissue [Ph.D. Dissertation]. Oulu, Finland: University of Oulu, 2002. Available online at: http://herkules.oulu.fi/isbn9514266900/index.html.
149. Shen Y, Lu Z, Spiers S, MacKenzie HA, Ashton HS, Hannigan J, Freeborn SS, Lindberg J: Measurement of the optical absorption coefficient of a liquid by use of a time-resolved photoacoustic technique. Appl Opt 2000;39:4007–4012.
150. Glucon, Inc.: Continuous non-invasive venous blood glucose monitor. A presentation at Diabetes Technology Meeting, Atlanta, November 2002. Available online at: www.Glucon.com.
151. Nagar R, Pesach B, Ben-Ami U, inventors: Photoacoustic assay and imaging system. US patent application 20030167002. September 4, 2003.
152. Hoelen CGA, de Mul FFM, Pongers R, Dekker A: Three-dimensional photoacoustic imaging of blood vessels in tissue. Opt Lett 1998;23:648–650.
153. Klonoff DC, Braig JR, Sterling BB, Kramer C, Goldberger DS, Trebino Y: Mid-infrared spectroscopy for non-invasive blood glucose monitoring. IEEE Laser Electro-Opt Soc Newslett 1998;12:13–14.
154. Zheng P, Kramer CE, Barnes CW, Braig JR, Sterling BB: Noninvasive glucose determination by oscillating thermal gradient spectrometry. Diabetes Technol Ther 2000;2:17–25.
155. Sterling BB, Braig JR, Goldberger DS, Kramer CE, Shulenberger AM, Trebino R, King RA, inventors; Optiscan Biomedical Corporation, assignee: Subsurface thermal gradient spectrometry. US patent 6,049,081. April 11, 2000.
156. Braig JR, Kramer CE, Sterling BB, Goldberger DS, Zheng P, Shulenberger AM, Trebino R, King RA, Barnes CW, inventors; Optiscan Biomedical Corporation, assignee: Method for determining analyte concentration using periodic temperature modulation and phase detection. US patent 6,556,850. April 29, 2003.
157. Buchert JM, inventor: Non-invasive continuous blood glucose monitoring. US patent 5,823,966. October 20, 1998.
158. Malchoff CD, Shoukri K, Landau JI, Buchert JM: A novel noninvasive blood glucose monitor. Diabetes Care 2002;25:2268–2275.
159. Sandby-Moller J, Poulsen T, Wulf HC: Influence of epidermal thickness, pigmentation and redness on skin autofluorescence. Photochem Photobiol 2003; 77:616–620.
160. Snyder WJ, Grundfest WS, inventors; Cedars-Sinai Medical Center, assignee: Glucose monitoring apparatus and method using laser-induced emission spectroscopy. US patent 6,232,609. May 15, 2001.
161. Russell RJ, Pishko MV, Gefrides CC, McShane MJ, Cote GL: A fluorescence-based glucose biosensor using concanavalin A and dextran encapsulated in a poly(ethylene glycol) hydrogel. Anal Chem 1999;71: 3126–3132.
162. McCartney LJ, Pickup JC, Rolinski OJ, Birch DJS: Near-infrared fluorescence lifetime assay for serum glucose based on allophycocyanin-labeled concanavalin-A. Anal Biochem 2001;292:216–221.
163. Rolinski OJ, Birch DJS, McCartney LJ, Pickup JC: Fluorescence nanotomography using resonance energy transfer: demonstration with a protein-sugar complex. Phys Med Biol 2001;46:N221–N226.
164. Evans ND, Gnudi L, Rolinski OJ, Birch DJ, Pickup JC: Non-invasive glucose monitoring by NAD(P)H autofluorescence spectroscopy in fibroblasts and adipocytes: a model for skin glucose sensing. Diabetes Technol Ther 2003;5:807–816.
165. Masters BR, So PT, Gratton E: Multiphoton excitation fluorescence microscopy and spectroscopy of in vivo human skin. Biophys J 1997;72:2405–2412.
166. Dong CY, Yu B, Kaplan PD, So PT: Performances of high numerical aperture water and oil immersion

objective in deep-tissue, multi-photon microscopic imaging of excised human skin. Microsc Res Tech 2004;63:81–86.
167. Swindle LD, Thomas SG, Freeman M, Delaney PM: View of normal human skin in vivo as observed using fluorescent fiber-optic confocal microscopic imaging. J Invest Dermatol 2003;121:706–712.
168. March WF, Ochsner K, Horna J: Intraocular lens glucose sensor. Diabetes Technol Ther 2000;2:27–30.
169. March WF: Apparatus for measuring blood glucose concentrations. Patent publication WO 2002087429 published under the International Patent Treaty.
170. Badugu R, Lakowicz JR, Geddes CD: Noninvasive continuous monitoring of physiological glucose using a monosaccharide-sensing contact lens. Anal Chem 2004;76:610–618.
171. Trepagnier P, Freeman J, Mansfield J, Brand D, Hopmeier MJ, Kollias N, inventors, Argose, Inc., assignee: Non-invasive tissue glucose level monitoring. US patent 6,721,582. April 13, 2004.
172. Holtz JH, Asher SA: Polymerized colloidal crystal hydrogel films as intelligent chemical sensing materials. Nature 1997;389:829–832.
173. Reese E, Baltusavich ME, Keim JP, Asher SA: Development of an intelligent polymerized crystalline colloidal array colorimetric reagent. Anal Chem 2001;73:5038–5042.
174. Asher SA, Sharma AC, Goponenko AV, Ward MM: Photonic crystal aqueous metal cation sensing materials. Anal Chem 2003;75:1676–1683.
175. Sharma AC, Jana T, Kesavamoorthy R, Shi L, Virji MA, Finegold DN, Asher SA: A general photonic crystal sensing motif: creatinine in bodily fluids. J Am Chem Soc 2004;126:2971–2977.
176. Alexeev VL, Sharma AC, Goponenko AV, Das S, Lednev IK, Wilcox CS, Finegold DN, Asher SA: High ionic strength glucose-sensing photonic crystal. Anal Chem 2003;75:2316–2323.
177. Asher SA, Alexeev VL, Goponenko AV, Sharma AC, Lednev IK, Wilcox CS, Finegold DN: Photonic crystal carbohydrate sensors: low ionic strength sugar sensing. J Am Chem Soc 2003;125:3322–3329.
178. Hillier TA, Abbott RD, Barrett EJ: Hyponatremia evaluating the correction factor for hyperglycemia. Am J Med 1999;106:399–403.
179. Caduff A, Hirt E, Feldman Y, Ali Z, Heinemann L: First human experiments with a novel non-invasive, non-optical continuous glucose monitoring system. Biosens Bioelectron 2003;19:209–217.
180. Jenkins PG, Larmors C: Hyperglycemia-induced hyponatremia. N Engl J Med 1974;290:573.
181. Ermolina I, Polevaya Y, Feldman Y: Analysis of dielectric spectra of eukaryotic cells by computer modeling. Eur Biophys J 2000;29:141–145.
182. Polevaya Y, Ermolina I, Schlesinger M, Ginzburg BZ, Feldman Y: Time domain dielectric spectroscopy study of human cells. II. Normal and malignant white blood cells. Biochim Biophys Acta 1999;1419: 257–271.
183. Hayashi Y, Livshits L, Caduff A, Feldman Y: Dielectric spectroscopy study of specific glucose influence on human erythrocyte membrane. J Phys D 2003;36:369–374.
184. Cho O-K, Holzgreve B, inventors; O-K Cho, assignee: Process and device for non-invasive determination of glucose in parts of the human body. US patent 5,795,305. August 18, 1998.
185. Cho OK, Holzgreve B, inventors; OK Kyung Cho, assignee: Process and device for determining the exchange of heat between the human body and the invented device and its correlation to the glucose concentration in human blood. US patent 5,924,996. July 20, 1999.
186. Ko JB, Cho OK, Kim YO, Yasuda K: Body metabolism provides a foundation for noninvasive blood glucose monitoring. Diabetes Care 2004;27:1211–1212.
187. Klonoff DC: The need for separate performance goals for glucose sensors in the hypoglycemic, normoglycemic, and hyperglycemic ranges. Diabetes Care 2004;27:834–836.

Address reprint requests to:
Omar S. Khalil, Ph.D.
Diagnostics Division
Abbott Laboratories
D9MS, AP 20
100 Abbott Park Road
Abbott Park, IL 60064

E-mail: Omar.khalil@abbott.com